



Cite this: *Biomater. Sci.*, 2022, **10**, 1166

## Non-viral delivery of the CRISPR/Cas system: DNA versus RNA versus RNP†

Yi Lin,<sup>a</sup> Ernst Wagner \*<sup>a</sup> and Ulrich Lächelt \*<sup>a,b</sup>

Since its discovery, the CRISPR/Cas technology has rapidly become an essential tool in modern biomedical research. The opportunities to specifically modify and correct genomic DNA have also raised big hope for therapeutic applications by direct *in vivo* genome editing. In order to achieve the intended genome modifications, the functional unit of the CRISPR/Cas system finally has to be present in the nucleus of target cells. This can be achieved by delivery of different biomolecular Cas9 and gRNA formats: plasmid DNA (pDNA), RNA or Cas9 ribonucleoproteins (RNPs). While the initial research focussed on pDNA transfections, the currently most promising strategy for systemic non-viral *in vivo* delivery is based on RNA which has achieved remarkable results in the first clinical trials. RNP delivery receives much attention for *ex vivo* applications, but the translation to systemic *in vivo* genome editing in patients has not been reached so far. The article summarises the characteristics and differences of each format, provides an overview of the published delivery strategies and highlights recent examples of delivery systems including the status of clinical applications.

Received 29th October 2021,  
Accepted 24th January 2022  
DOI: 10.1039/d1bm01658j  
[rsc.li/biomaterials-science](http://rsc.li/biomaterials-science)

## Introduction

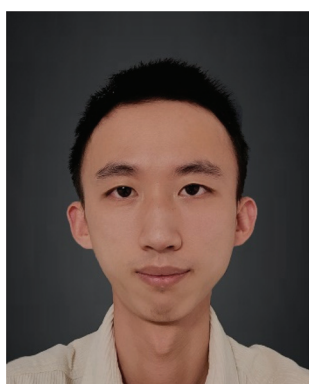
The CRISPR/Cas9 system, which was initially discovered as a type of adaptive immune system in bacteria,<sup>1</sup> revolutionized

biomedical research due to the applicability as a programmable endonuclease.<sup>2</sup> The genome editing tool is composed of the endonuclease Cas9 and a guide RNA (gRNA) which guides the protein to the target DNA sequence followed by a protospacer adjacent motif (PAM). The double-stranded DNA is unwound and a double-strand break (DSB) introduced 3–4 base-pairs upstream of the PAM sequence. The cellular machinery repairs DSBs in genomic DNA primarily *via* two distinct pathways (Fig. 1), non-homologous end joining (NHEJ) and homology directed repair (HDR).<sup>3,4</sup> NHEJ represents the direct re-ligation of the cleaved DNA strands without involve-

<sup>a</sup>Department of Pharmacy and Center for NanoScience (CeNS), Ludwig-Maximilians-Universität München, Munich, Germany. E-mail: ernst.wagner@lmu.de, ulrich.laechelt@univie.ac.at

<sup>b</sup>Department of Pharmaceutical Sciences, University of Vienna, Vienna, Austria

†Electronic supplementary information (ESI) available. See DOI: 10.1039/d1bm01658j



Yi Lin

Yi Lin received his Master's degree in Pharmaceutics from National Engineering Research Center for Biomaterials (NERCB), Sichuan University, China in 2018. He is currently pursuing his Ph.D. at the Department of Pharmacy, Ludwig-Maximilians-Universität (LMU) München under the supervision of Prof. Ulrich Lächelt and Prof. Ernst Wagner. The current research of him focuses on the development of artificial oligoaminoamide peptides for Cas9/sgRNA ribonucleoprotein delivery and cancer therapy.

aminoamide peptides for Cas9/sgRNA ribonucleoprotein delivery and cancer therapy.



Ernst Wagner

Ernst Wagner is professor of Pharmaceutical Biotechnology at LMU and Center of Nanoscience since 2001. Previously he was Director Cancer Vaccines, Boehringer Ingelheim (first polymer-based gene therapy trial), group leader at IMP Vienna, postdoc at ETH Zurich and received a PhD in chemistry (TU Vienna) in 1985. He is Academician of European Academy of Sciences, member of College of Fellows of the Controlled Release Society, board of German Society for Gene Therapy and has authored 486 publications.

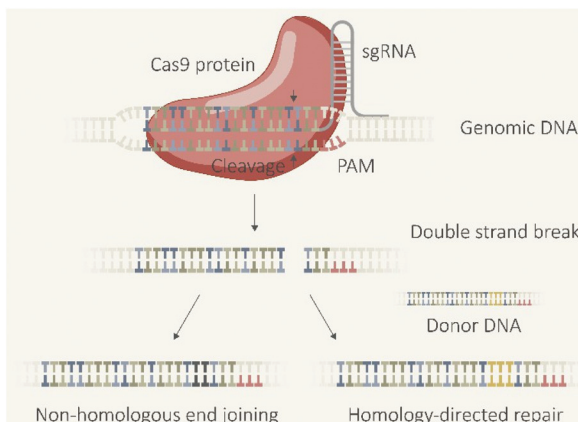


Fig. 1 Mechanisms of CRISPR-Cas9 genome editing.

ment of a homologous DNA template. This error prone mechanism can lead to random insertions and deletions of nucleotides (indels) at the cleavage site which in part result in frame-shift mutations and target gene knockout. In presence of a DNA template with homologous flanks, HDR mediates an accurate repair and the insertion of a defined DNA sequence, embedded between the homology arms at the cleavage site, can be realized. These strategies of using the cellular DSB repair machinery for introducing gene knock-outs or knock-ins are generally independent of the utilized endonuclease. However, the flexible control over the sequence recognition by simple variation of the gRNA component explains the uniqueness of CRISPR/Cas9 compared to other genome editors, such as transcription activator-like effector nucleases (TALENs) or zinc finger nucleases (ZFNs), which require individual protein design for each alteration of the target site.<sup>5</sup> The functional unit of the CRISPR/Cas system is represented by the Cas9/gRNA ribonucleoprotein (RNP) complex which has to reach the nucleus of eukaryotic cells (eventually together with template

DNA) for mediating the intended genomic modifications. To achieve this, different biomolecular formats can be selected and utilized for cellular delivery: plasmid DNA (pDNA) encoding for the Cas9 protein and the specific guide RNA (gRNA); a mixture of Cas9 mRNA and gRNA; or the pre-assembled RNP complex. Each strategy has its own features, prerequisites, advantages or drawbacks. This review presents approaches for the cellular delivery of the different biomolecular CRISPR/Cas9 formats and highlights their differences and characteristics.

## Molecular basis of DNA, RNA and protein transfer

To achieve intended genome modifications with the CRISPR/Cas system, the RNP complex has to be present in the nucleus of target cells. In general, the artificial introduction of exogenous proteins into cells can be achieved by different strategies: direct cellular transport of the protein of interest, or deposition of genetic 'blue prints' which induce production of the foreign protein by the cellular machinery. As 'blue prints' based on the universal genetic code, DNA expression cassettes and mRNA can be used to trigger the protein production. Although both types of nucleic acids can achieve the same result, their application differs due to the involved biological mechanisms and individual characteristics. To understand the potential implications of different biomolecular formats on genome editing, the general characteristics and molecular basis of DNA, RNA and protein delivery are discussed first.

### DNA

Plasmid DNA (pDNA) is generally used as vector for non-viral DNA delivery, since the circular pDNA is not prone to degradation by exonucleases, can be complexed by common transfecting agents in more condensed form, is internalized into cells more efficiently and consequently achieves higher transgene expression than linear DNA constructs.<sup>6,7</sup> The latter are mostly used, if a stable integration into the host genome is intended which preferentially occurs *via* homologous recombination of DNA with free ends, even though genome insertion can also occur with transferred pDNA at a rather low frequency. A technical advantage of pDNA is its facile and convenient production *via* amplification in bacteria. The other side of the coin is that bacterial backbone elements, such as a prokaryotic origin of replication, antibiotic resistance genes and unmethylated CpG motifs, can provoke immune reactions and short-lived transgene expression. To overcome this drawback, circular DNA constructs, only containing the expression cassette for the gene of interest (minicircle DNA), can be generated resulting in a smaller size, lower immunogenicity and longer persistence of transgene expression.<sup>8,9</sup> Consistent with the flow of genetic information inside our cells, DNA first has to enter the nucleus for being transcribed into the corresponding mRNA, which is then translocated to the cytosol.



Ulrich Lächelt

*Ulrich Lächelt is an assistant professor at the Department of Pharmaceutical Sciences of the University of Vienna since 2021. He studied pharmaceutics at the University of Heidelberg, received the degree of Doctor of Natural Sciences in the field of Pharmaceutical Biology at the LMU Munich in 2014 and was a group leader at the Chair of Pharmaceutical Biotechnology until his appointment at the University of Vienna. His research focuses on the intracellular delivery of biomolecules and the development of nanopharmaceuticals based on inorganic-organic hybrid materials.*



## RNA

By using mRNA as genetic 'blue print', the first steps of nuclear translocation and transcription can be omitted and the mRNA is directly translated by the ribosomes in the cytosol. As a result, mRNA transfer leads to a faster kinetic and earlier onset of protein expression in a higher number of cells compared to pDNA transfactions. Single-cell analysis studies showed that the onset of protein expression occurs within a narrow time window a few hours after mRNA transfaction, whereas pDNA transfactions exhibit a higher variance of expression onset time in different cells, presumably due to the cell cycle dependence of nuclear translocation (Fig. 2).<sup>10</sup> This also explains that the delivery of mRNA into non-dividing cells is generally more efficient, since the nuclear entry of pDNA is favored during the mitotic breakdown and reformation of the nuclear envelope.<sup>11,12</sup> The reproducible and controllable nature of mRNA expression even enables approximation of intracellular pharmacokinetics represented by the area under the curve (AUC) of the intracellular protein product (Fig. 3).<sup>13</sup>

Already in the 1960s Smull *et al.*, Vaheri and Pagano reported the use of histone, protamine sulfate and diethylaminoethyl dextran to enhance the infectiousness of viral RNA, which can be considered historical first nucleic acid transfactions.<sup>14,15</sup> In 1990, Wolff *et al.* published the first example of *in vivo* protein expression upon mRNA injection in mice.<sup>16</sup>

Although the utilization of mRNA as protein encoding nucleic acids has obvious advantages and first reports about RNA transfer *in vitro* and *in vivo* were known for decades, the research field required considerable time to establish suitable technologies and to show general feasibility of the approach. With the approval and extensive application of mRNA-based

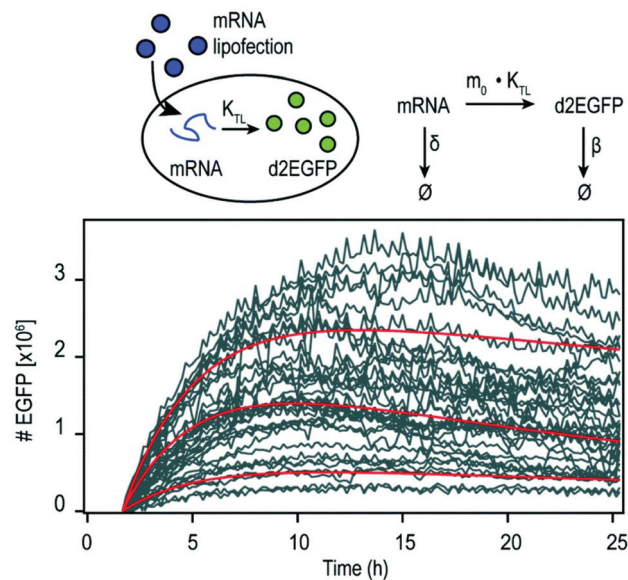


Fig. 3 Pharmacokinetics of mRNA transfactions. Top: Illustration of cellular mRNA lipofection and the reaction scheme describing underlying pharmacokinetic processes. Bottom: Exemplary time-courses of mRNA-mediated d2EGFP expression in A549 cells derived from micropattern-based single-cell arrays. The pharmacokinetics of intracellular protein production can be described by  $AUC = 0.48 \times m_0 \times k_{TL} \times \tau_{mRNA} \times \tau_{Protein}$  where  $AUC$  is the cumulative time-dose of the protein,  $m_0$  is the applied mRNA dose,  $k_{TL}$  is the translation efficiency, and  $\tau$  is the half-life of the mRNA or protein, respectively. Reproduced from ref. 13 under the terms of the Creative Commons CC BY-NC 3.0 License (2015).

COVID-19 vaccines in 2021, the outstanding potential of mRNA transfer has finally been demonstrated impressively. Major hurdles for the development of mRNA-based therapeutics were the high innate immunogenicity of exogenous mRNA due to activation of Toll-like receptors, as well as a general low chemical stability and high nuclease sensitivity of RNA which are intrinsic properties of this particular type of nucleic acids.<sup>17,18</sup> While DNA is the biological medium for long term storage of genetic information, RNA mainly serves as transient transmitter or regulator with a short half-life in biological fluids of only a few minutes. The group of Remaut investigated the decay kinetics of pDNA and mRNA and determined a half-life in biological samples of approximated 1–2 minutes for mRNA and 1–4 hours for pDNA (Fig. 4A).<sup>19</sup> In fact, a high mRNA turnover rate, as a result of the interplay between regulated RNA synthesis and fast degradation, is essential to generate a dynamic transcriptome and keep cellular homeostasis. However, this makes clear, why the gene therapy research initially focused on the transfer of DNA, with higher stability and longer half-life, instead of RNA. This changed with the technological innovations and the development of chemically modified and codon-optimized mRNA with low immunogenicity, tuneable stability and high translatability.<sup>20,21</sup> Heissig *et al.* used fluorescence lifetime imaging microscopy to assess the intracellular degradation of FRET-pair labelled short RNA oligonucleotides with different

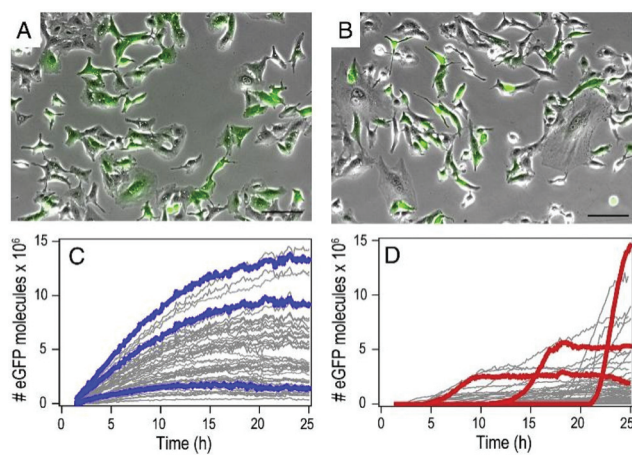
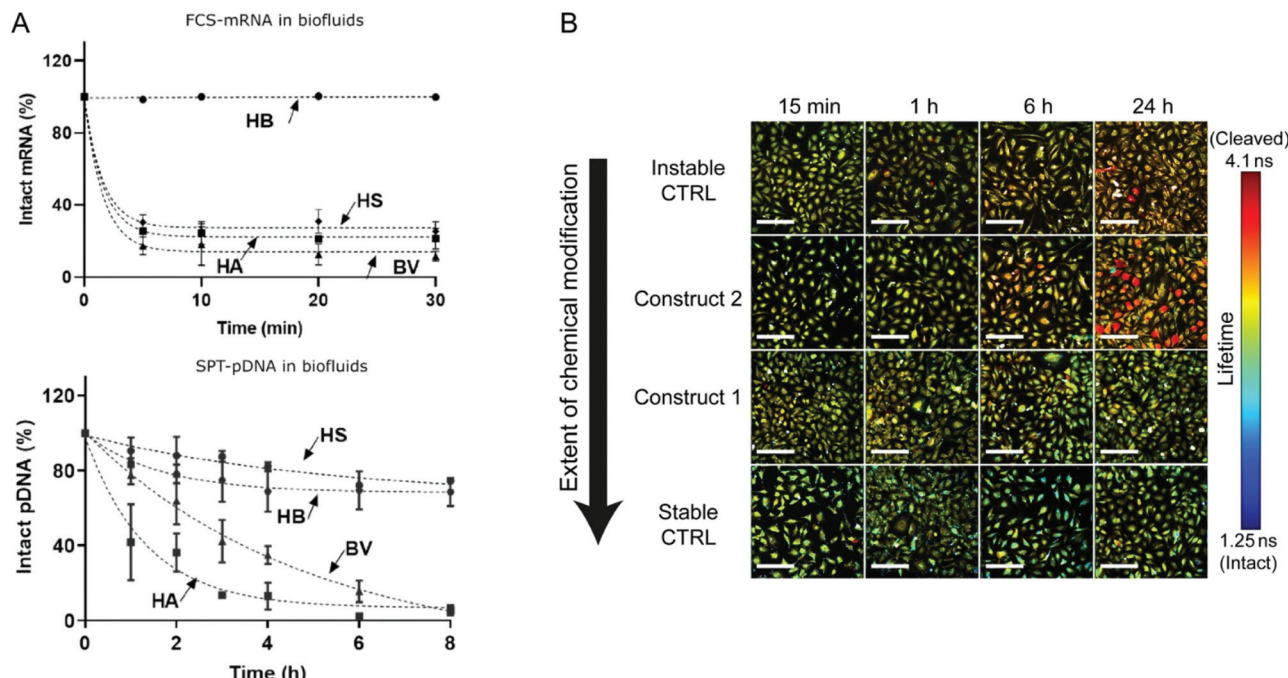


Fig. 2 mRNA- and pDNA-mediated GFP expression kinetics in A549 cells. (A and B) Exemplary fluorescence microscopy images 25 h after transfection. (C and D) Representative GFP fluorescence time-courses after mRNA (C) and pDNA (D) transfactions determined by single-cell analysis. mRNA transfactions mediate early onset and continuous increase of GFP fluorescence, whereas pDNA transfactions show less homogenously timed expression in different cells. Reproduced from ref. 10. Copyright (2014), with permission from Elsevier.





**Fig. 4** (A) Kinetics of mRNA and pDNA degradation in biological fluids. HEPES buffer (HB), human serum (HS), human ascites (HA), and bovine vitreous (BV) at 37 °C. Top: mRNA decay as determined by fluorescence correlation spectroscopy. Bottom: Cy5-pDNA decay as determined by single particle tracking analysis. Reproduced with permission from ref. 19. Copyright 2020 Wiley-VCH GmbH. (B) Intracellular integrity of single stranded RNA molecules in dependence of chemical modifications visualized by fluorescence life time imaging. Reproduced with permission from ref. 22 under the terms of the Creative Commons CC BY 4.0 License (2017).

chemical modification patterns (phosphorothioate, 2'-O-Me, 2'-F).<sup>22</sup> After transfection into HeLa cells, the intracellular integrity of the different oligonucleotides was monitored over time and a clear correlation with the extent of modification was confirmed (Fig. 4B).

### Proteins

The direct delivery of proteins of interest represents an obvious strategy to achieve well controllable introduction into cells. Considering the intracellular pharmacokinetics, direct protein delivery achieves instantaneous availability without requirement of gene expression or mRNA translation and the duration of persistence only depends on the degradation of the protein. Protein degradation in eukaryotic cells mainly occurs *via* the ubiquitine-proteasome system or proteolysis in lysosomes and the half-lives of different proteins vary significantly (Fig. 5). Therefore, the kinetic of intracellular availability can be expected to simplify to a dependency on the two parameters of protein dose and half-life, described by the exponential decay equation (Fig. 5A).<sup>23</sup>

### Intracellular delivery

Despite the differences in the molecular biology of pDNA and mRNA, the two types of nucleic acids share high similarity in their chemical composition on the sub-molecular level and their physicochemical properties are dominated by the negatively charged phosphate backbones. With the exception of

physical entrapment in liposomes or porous nanoparticles, co-precipitation and biomimetication strategies, most non-viral pDNA and mRNA delivery system are based on the electrostatic interaction with positively charged groups of the delivery systems. Cationic or cationizable oligo- and polymers, lipids and lipidoids have intensely been used for the transfer of pDNA and mRNA into cells. Also, the lipid nanoparticle (LNP) formulations of the COVID-19 mRNA vaccines contain cationizable lipids as essential component. Despite nucleic acid binding, these serve an additional essential purpose within the LNP delivery system: the amino-function of the lipid, with specific  $pK_a$  around 6, is protonated in the acidic environment of endosomes, which triggers a conformational change, disruption of the endosomal membrane and release of the internalized material into the cytosol. This 'endosomal escape' is a generally critical step within the cellular delivery pathway and has to be addressed by all systems which are internalized *via* an endocytic uptake mechanism. Also most polymeric transfecting agents rely on a specific protonation in the endosomal environment. Polyethylene imine (PEI), which is utilized for pDNA transfections since the 1990s, is characterized by a broad protonation range, including the endosomal pH, due to the highly repetitive diaminoethane motif.<sup>24</sup> The discovery of the chemical principle and favourable consequences for cellular gene transfer, made PEI an archetype of polymeric transfecting agents and inspired scientists around the world to include PEI-like motifs into more defined and better tolerated

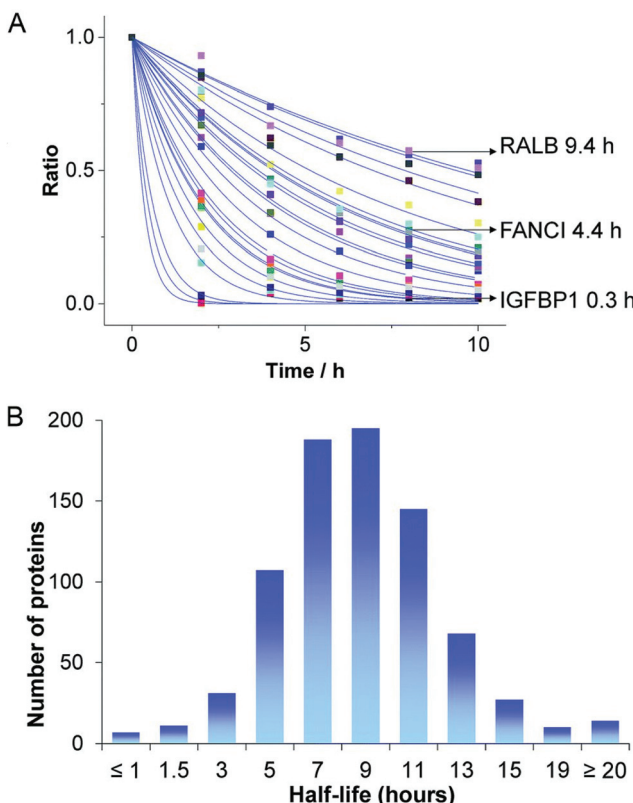


**Fig. 5** Degradation of endogenous proteins. (A) Abundance changes of different endogenous proteins and (B) the distribution of protein half-lives. The kinetic of intracellular protein degradation can be described by  $P = P^0 e^{-kt}$ , where  $P$  is the abundance of the protein at each time point  $t$ ,  $P^0$  is the initial protein availability and  $k$  is the degradation rate constant. Reproduced from ref. 23 under the terms of the Creative Commons CC BY 3.0 License (2016).

delivery systems. By dissecting the chemical structure of PEI into shorter oligoamine segments, the relevance of specific protonation characteristics and the relation to biological activity became unveiled, while cytotoxicity was frequently reduced.<sup>25–31</sup>

Early demonstrations of intracellular protein delivery by chemical carriers were reported in the 1970s based on liposomes.<sup>32,33</sup> In contrast to nucleic acids which are, despite the existence of different types, relatively similar in their chemical composition and physico-chemical properties, proteins are an extremely diverse class of biomolecules. They vary in size, structural conformation, charge and hydrophilicity/hydrophobicity. Therefore, the development of generic strategies for protein delivery is sophisticated, and in many cases individual carrier design and optimization are required. Despite physical entrapment in liposomes, conjugation of cell penetrating peptides (CPPs) or protein transduction domains (PTDs)<sup>34–36</sup> as well as nanomicelles,<sup>37–39</sup> engineered nanocarriers<sup>40,41</sup> and other strategies have been used for cellular protein delivery. Since classic nucleic acid transfecting agents, cationic polymers or lipids, generally only work with negatively charged proteins, a very flexible strategy is rep-

resented by charge-conversion. Here, the positively charged amino groups in proteins are reversibly converted into negatively charged functions, for instance *via* reaction with citraconic or *cis*-aconitic anhydride.<sup>42</sup> The resulting protein derivatives with multiple negative charges are then susceptible for the electrostatic interaction and delivery by cationic transfecting agents. A similar aim is achieved by the genetic engineering of negatively charged protein analogs by fusion with supercharged proteins or peptide tags, which can enable electrostatic complexation by cationic delivery agents.<sup>43,44</sup>

Table 1 gives an overview over the different biomolecular formats for the introduction of exogenous proteins into cells and summarizes their properties and characteristics.

## Physicochemical and physiological characteristics of different CRISPR/Cas9 formats

### Cas9 plasmid DNA

Typical and well-established SpCas9 plasmids for transfection of mammalian cells are pX260 and pX330 from the Zhang laboratory. pX260 is an older CRISPR/Cas plasmid system, which contains three expression cassettes; one is used to drive SpCas9 nuclease expression and the other two are used to express the CRISPR RNA array and tracrRNA.<sup>45</sup> At present, the most commonly used SpCas9 plasmid is pX330 that contains only two expression cassettes, a human codon-optimized SpCas9 and a chimeric single guide RNA. It has 8484 bp with  $1.68 \times 10^4$  negative charges and a molecular weight of around  $5.24 \times 10^3$  kDa. Generally, the pX330 vector can be digested by the restriction enzyme BbsI to insert a pair of annealed oligonucleotides that are designed based on the specific target site (20 bp) upstream of the NGG PAM sequence. Larger plasmid constructs containing an additional reporter gene (e.g. pX458 encoding GFP) to identify and enrich transfected cells, or a selection marker (e.g. pX459 encoding resistance to puromycin) to generate stable cell lines are also available.<sup>45</sup>

### Cas9 mRNA and sgRNA

Different from the two-in-one Cas9 plasmids, co-delivery of two individual components, Cas9 mRNA and sgRNA, is required in case of RNA-based strategies of the CRISPR/Cas system. Cas9 mRNA with the length of approximately 4500 nt is a linearized single-stranded RNA which is produced *via* *in vitro* transcription (IVT) followed by 5' capping and 3' poly-A modification.<sup>46,47</sup> The 5' capping of IVT mRNA mimics the natural eukaryotic mRNA which has a 7-methylguanosine (m7G) cap at the 5' end.<sup>48</sup> It can protect the mRNA against exonuclease degradation and assists in eukaryotic initiation factor (eIF) 4E recognition and binding during translation.<sup>49</sup> The poly-A tail is a long chain of adenine nucleotides. It is added to the 3' end of the mRNA transcript to increase its enzymatic stability, and it can act synergistically with the 5' m7G cap to regulate translation efficiency as well as enhance protein



**Table 1** Characteristics and properties of biomolecular formats for the introduction of exogenous proteins into cells

	pDNA	mRNA	Protein
Production Size	Bacterial amplification ≈ 2.000 <sup>a1</sup> –300.000 bp <sup>a2</sup> (≈ 1.200–185.000 kDa)	<i>In vitro</i> transcription ≈ 500–100.000 nt <sup>a3</sup> (≈ 160 kDa–32.000 kDa)	Recombinant expression or isolation ≈ 50–30.000 aa <sup>a4</sup> (≈ 5–4000 kDa)
Properties and appearance Stability	Double-stranded DNA, circular, negatively charged, hydrophilic Relative chemical stability, nucleolytic instability	Single-stranded RNA, linear, negatively charged, hydrophilic High chemical and nucleolytic instability	Diverse (molecular weight, charge, isoelectric point, hydrophilicity, etc.) Proteolytic instability, sensitivity to denaturation depending on individual protein
Kinetic	Variable onset of protein expression, cell cycle dependence, long duration of persistence possible	Fast and homogenous onset of protein expression, short duration of persistence	<i>Ab initio</i> availability of protein, minimal duration of persistence (dependent on protein half-life)
Individual problems	Risk of genome integration, potential immunogenicity due to bacterial sequences (not for minicircle DNA)	Chemical modifications required to increase stability and reduce immunogenicity	Potential immunogenicity, protease sensitivity, no generic delivery technologies for all kind of proteins
Delivery technologies	Ionic interaction with cationic polymers or lipids, encapsulation in or adsorption to inorganic nanoparticles		Conjugates (CPPs, polymers), encapsulation into micelles or liposomes, ionic interaction of negatively charged or charge-converted proteins with cationic polymers or lipids, encapsulation in or adsorption to inorganic nanoparticles

<sup>a</sup>The specified size limits of pDNA, mRNA and proteins are based on the considerations of: 1: minicircle DNA; 2: bacterial artificial chromosomes (BAC) as well as 3: the largest human protein titin and 4: the corresponding mRNA transcript.

expression.<sup>50,51</sup> With regard to mRNA stabilization, introduction of phosphorothioates especially into the 5' untranslated mRNA sequence has been shown to increase protein translation and to result in up to 22-fold enhanced protein expression.<sup>52</sup> Generally, endocytosed IVT mRNA can be recognized by several endosomal innate immune receptors (TLR3, TLR7 and TLR8) and cytoplasmic proteins such as melanoma differentiation-associated protein 5 (MDA5) and retinoic acid inducible gene I protein (RIG-I), which may induce immune responses and inhibit the function of mRNA.<sup>17,53,54</sup> The intrinsic immune activation activity of IVT mRNA is usually considered beneficial for immunotherapeutic vaccination, but a major disadvantage for non-immunotherapy-related applications since the induced immune responses can slow down the translation of mRNA and promote RNA degradation.<sup>53,54</sup> Incorporation of chemically modified nucleotides, such as 2-thiouridine (s2U), 5-methyluridine (m5U), pseudouridine (Ψ), N<sup>1</sup>-methylpseudouridine (m1Ψ), 5-methylcytidine (m5C), 5-hydroxymethylcytosine (5hmC), into mRNA sequences are the mostly used strategies to overcome the high immunogenicity of IVT mRNA.<sup>20,55–57</sup> Besides, some studies showed that lower immunogenicity can be achieved by sequential engineering and the use of high-performance liquid chromatography (HPLC)-purified mRNA.<sup>58,59</sup>

Another key component of the RNA-based strategy is the sgRNA which has a smaller size of approximately 100 nt. sgRNA can either be generated by IVT or, due to the much shorter length, by solid-phase synthesis.<sup>60,61</sup> IVT is a widely used approach for sgRNA production, since it is cost-effective, high-yielding and easy to implement. On the other hand, IVT sgRNA can be expected to face similar problems as other IVT generated RNA products, such as IVT mRNA, which could limit its applicability *in vivo*. Firstly, IVT RNA contains diverse variants with different lengths and structures which may cause

variable and inconsistent editing efficiencies.<sup>53,62</sup> Secondly, the stability of unmodified IVT RNA generally is not favourable for *in vivo* usage.<sup>63</sup> Even if modified nucleotides are used for the IVT reaction, random incorporations of the nucleotides into the RNA sequence can still be a non-negligible issue.<sup>64</sup> With regards to the CRISPR/Cas system, it has been reported that IVT sgRNA can induce immune responses and even cause cell apoptosis.<sup>65–67</sup> In contrast to IVT sgRNA, chemically synthesized sgRNA is structurally well-defined and homogenous. Synthetic sgRNA which lacks a 5'-triphosphate group is less immunogenic and does not induce detectable immune response in many cell types.<sup>66–68</sup> Moreover, the chemical oligonucleotide assembly enables site-specific incorporation of modified nucleotides during solid-phase synthesis. Various chemically modified nucleotides, including 2'-methyl (M), 2'-O-methyl-PS (MS), 2'-O-methyl-3'-thiophosphonoacetate (MSP), phosphorothioates, 2'-fluoro (F), 2'-O-methyl-3'-phosphonoacetate (MP), locked nucleic acids (LNA) and bridged nucleic acids (BNA), are developed to enhance the enzymatic stability, editing efficiency, specificity as well as to reduce the immunogenicity and off-target effects of sgRNA.<sup>69–77</sup>

### Cas9/gRNA ribonucleoprotein (RNP)

Similar to the RNA strategy, protein-based delivery of the CRISPR/Cas system also requires two critical components in the formulation: the Cas9 nuclease and a guide RNA (gRNA). But in contrast to the mRNA-based strategy, which requires co-delivery of the discrete mRNA and sgRNA species, the Cas9 protein is first pre-complexed with gRNA to form the negatively charged Cas9/gRNA ribonucleoprotein (Cas9 RNP) complex, which can then be delivered as one single cargo entity. The typical SpCas9 protein comprises 1368 amino acids with a molecular weight of 158.4 kDa and a net positive charge of +22.<sup>44,78</sup> The structure of the SpCas9 protein exhibits two



lobes: an  $\alpha$ -helix recognition lobe (REC) and a nuclease lobe (NUC).<sup>79</sup> These two lobes are linked by the arginine-rich bridge helix (Arg) and the disordered linker (DL).<sup>79</sup> The NUC lobe contains a RuvC domain and a HNH nuclease domain for cleavage of the target DNA, as well as a C-terminal domain (CTD) for recognizing the PAM sequence.<sup>79</sup> The REC lobe consists of three  $\alpha$ -helical domains and plays a vital role in recognition of DNA, regulation of conformational transition of the HNH nuclease domain and directing HNH to the cleavage site.<sup>79,80</sup>

As gRNA component for Cas9 RNP assembly, two different variants can be utilized: (1) a crRNA:tracrRNA duplex, or (2) a single guide RNA (sgRNA). The two-component guide RNA represents the naturally occurring form of the bacterial CRISPR/Cas9 system and comprises a CRISPR RNA (crRNA) with a custom 20 nt targeting sequence and a trans-activating crRNA (tracrRNA), which is crucial for Cas9 recruitment.<sup>81</sup> sgRNA is created by fusing the crRNA and tracrRNA sequences *via* a scaffold loop into a single RNA chimera, which became the most popular format for RNP-based CRISPR delivery. In the absence of gRNA, the Cas9 protein remains in an inactive conformation.<sup>82</sup> When it is bound to gRNA, the REC lobe undergoes a conformational change which converts the inactive protein into the active RNP form.<sup>79,82</sup> Since the binding of gRNA is highly associated with the functional domains of the Cas9 protein, the types and positions of modified nucleotides need to be carefully selected to avoid a potential interference with RNP formation. A very special feature of Cas9 RNPs, with high relevance for delivery, is the charge-conversion of the positively charged Cas9 protein upon binding of the negatively charged sgRNA component. The work by Zuris *et al.* on genetically engineered supercharged proteins demonstrated, that the sgRNA component in Cas9 RNPs already provides sufficient negative charge for the delivery with cationic lipids.<sup>44</sup> Kuhn *et al.* reported the cellular delivery of Cas9 RNPs with oligoaminoamides, containing lipid-modifications and stabilizing tyrosine trimers,<sup>83</sup> and determined by fluorescence correlation spectroscopy that the cationic oligomers only interact with fluorescently labelled Cas9, if the negatively charged sgRNA has been loaded.<sup>84</sup> These results illustrate a significant characteristic of Cas9 RNPs which provides the basis for cellular delivery by cationic transfecting agents without requirement of protein derivatization or individual nanocarrier design.

### Comparison of different formats of CRISPR/Cas9

Since each format has its intrinsically unique physicochemical and physiologic features, it is crucial to understand how these features affect the Cas9 action process and then select the best format for practical applications. The most direct distinction is the stability. Cas9 plasmid DNA (Cas9 pDNA) possesses the highest stability among the three formats. Chemically, DNA contains deoxyribose while RNA contains ribose. The absence of the single hydroxyl group in 2' position of the pentose ring makes DNA more stable and less reactive than RNA.<sup>85</sup> Moreover, Cas9 pDNA is a circular double-stranded DNA which is not vulnerable to exonucleases.<sup>86,87</sup> Although Cas9 mRNA is

more fragile than Cas9 pDNA, chemical modifications on the nucleotides can be applied to improve the stability as mentioned above.<sup>63,88</sup>

Compared to pDNA and mRNA, which contain only a single type of biomolecules, Cas9 RNPs consist of protein and sgRNA and are susceptible to degradation by both proteases and RNases, hypothetically making it the least stable format. Besides, the Cas9 protein may not be resistant to organic solvents and is easily denatured. For example, denaturation of Cas9 RNP is observed in acidic citrate buffer at pH 4.0, which represent standard conditions for the formulations of nucleic acid loaded LNPs.<sup>89</sup>

Another obvious difference is the place of action. As discussed in the previous section, nuclear entry is an essential prerequisite for the transfer of pDNA. In contrast, Cas9 mRNA only requires delivery to the cytoplasm where the translation process may start immediately. However, in both cases, the RNP complex has to be assembled with gRNA after the Cas9 protein has been produced, which inevitably results in a certain latency between the intracellular availabilities of the protein and RNA components. In this regards, delivery of *a priori* formed functional RNPs is the most direct way for cellular genome editing, which generally is also considered the most efficient strategy.<sup>90</sup> As a last step, the Cas9 RNP has to enter the nucleus to reach its target site and for this reasons nuclear localization signal (NLS)-fused Cas9 is commonly used.<sup>91</sup> As discussed above, the duration of intracellular persistence depends on the stability of the genetic 'blue prints' and degradation of encoded protein. For genome editing applications, the CRISPR/Cas components are only transiently required until the intended genome modification has occurred; an additional presence in the cell generally is not favored, since the risk of off-target events can increase with the duration of presence in the cell. Therefore, a high control over the availability of the functional CRISPR/Cas system and a degradation or inactivation after the intended task has been fulfilled, are desirable. Due to the more rapid degradation within the target cells, Cas9 RNP and mRNA provide a shorter exposure time of the cellular genome to active Cas9 proteins and decrease the potential risk of off-target effects.<sup>92,93</sup> In contrast, Cas9 pDNA can mediate longer gene expression that may increase off-target editing events.<sup>94</sup>

Independent of the biomolecular format, additional strategies to minimize mutations at unintended sites include shortening Cas9 half-life by tagging with degradation signals,<sup>95,96</sup> reducing Cas9 activity by coupling to inhibitory domains,<sup>97</sup> or selective activation of Cas9 variants by external triggers such as chemical reagents<sup>98,99</sup> or light.<sup>100</sup> In addition, other Cas9 variants have been designed to optimize the on/off-target ratio, such as catalytically inactive Cas9 fused to the catalytic domain of the endonuclease FokI (dCas9-FokI),<sup>101</sup> mutated variants with attenuated activity at mismatch targets, such as high-fidelity Cas9 (SpCas9-HF1),<sup>102</sup> enhanced specificity Cas9 (eSpCas9),<sup>103</sup> hyper-accurate Cas9 (HypaCas9),<sup>104</sup> evoCas9,<sup>105</sup> Sniper-Cas9<sup>106</sup> and expanded PAM SpCas9 (xCas9).<sup>107</sup> Nickases, generated by deactivation of the nucleolytic RuvC

(Cas9-D10A) or HNH (Cas9-H840A) domain, induce single-strand nicks instead of double-strand breaks and therefore require a pair of gRNAs for gene disruption, which strongly increases the specificity.<sup>2,45,108</sup>

Apart from their stability and action features, safety is a major concern, especially considering potential *in vivo* applications. As stated above, random integration of Cas9 pDNA into the host genome may cause potentially harmful insertional mutagenesis as well as persistent Cas9 expression that can lead to off-target effects and MHC class I immune responses.<sup>92,109</sup> In this regard, Cas9 RNP and mRNA appear as the safer choices for genome editing. Besides, the main type of immune response induced by these three formats is also different. Cas9 pDNA and mRNA mainly trigger innate immune responses by activating Toll-like receptors (TLRs), while Cas9 RNP can induce adaptive immune reactions.<sup>109–113</sup> Recent studies have demonstrated that anti-Cas9 antibodies and T cells are pre-existing due to preceding bacterial infections.<sup>109,112,113</sup> IgG antibodies against SpCas9 and anti-SpCas9 T cells were detected in 58% and 67% of human adults, respectively.<sup>109</sup>

Although Cas9 mRNA and RNP have certain advantages in terms of editing efficiency and safety, the costs are generally higher than for pDNA, since pDNA design, production and scale up are more feasible. In contrast, obtaining pure active Cas9 proteins is a time-consuming and complex process, which includes a series of critical steps, such as protein isolation from bacterial cultures, purification, suitable storage of

the sensitive protein product *etc.*<sup>114</sup> Notably, endotoxin contamination could occur during both pDNA and Cas9 protein preparation, while the cell-free mRNA production exhibits a much lower risk. Finally, the clinical translation of nucleic acid-based therapeutics is more mature than intracellular delivery of proteins, which is impressively demonstrated by the recent success of siRNA-based drugs and mRNA vaccines.<sup>115,116</sup> To sum up this section, the individual CRISPR/Cas9 formats differ in their physicochemical properties, stability, action features, safety and production. Fig. 6 presents a summary of the distinction and individual characteristics. Notably, none of these formats can work without a suitable and efficient delivery technology. Therefore, the delivery strategies utilized for pDNA, mRNA and RNP-based CRISPR/Cas9 systems are reviewed in the following section.

#### Non-viral delivery of different CRISPR/Cas9 formats

Up to now, various delivery strategies have been utilized for the delivery of the CRISPR/Cas9 system, which can be categorized into three general classes: (1) physical methods, (2) viral vectors, and (3) non-viral vectors.<sup>117</sup> Several of these systems have already been utilized for *ex vivo* gene therapy approaches by applying genome editing to patient cells in clinical studies<sup>118</sup> and technologies have been tested in direct *in vivo* applications, including systemic administration to patients.<sup>119</sup> This article focusses on the non-viral vectors which are generated from diverse synthetic and bioderived materials. In general, each vector is designed for one specific Cas9 format,

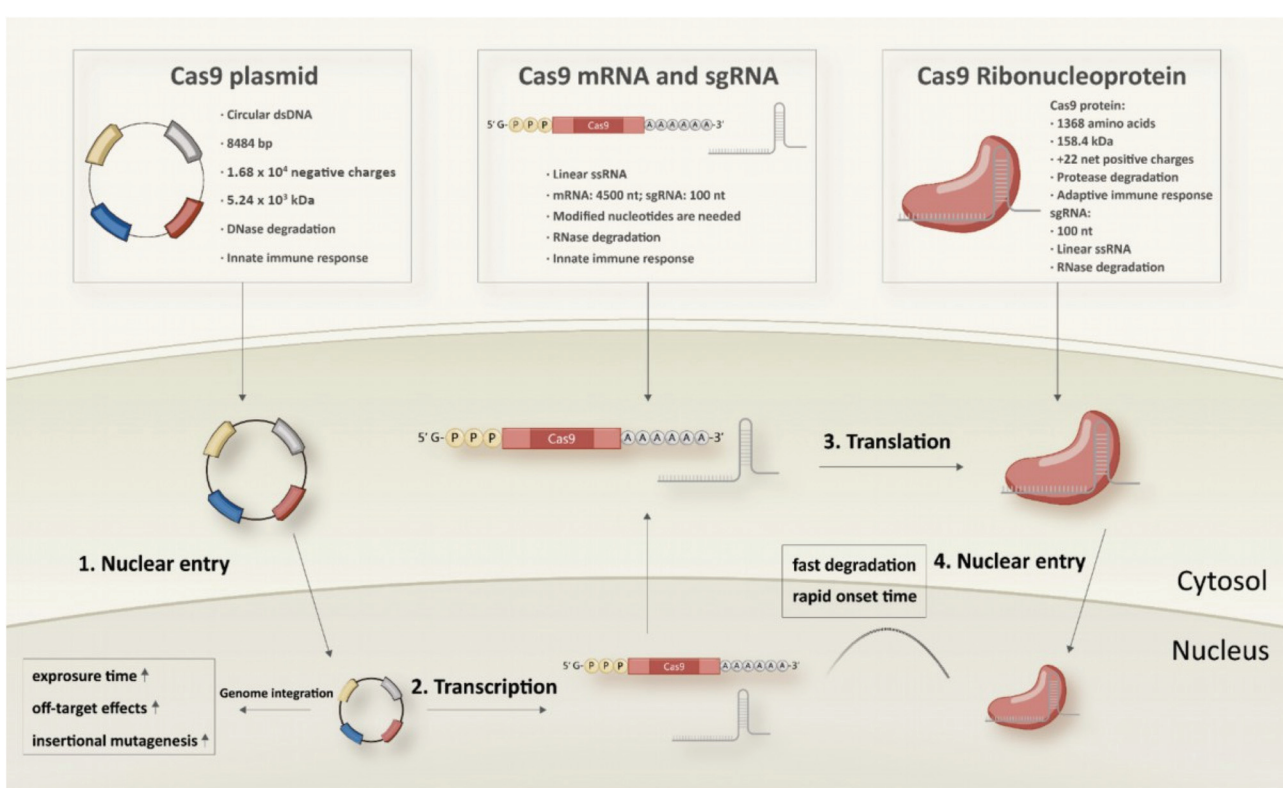


Fig. 6 Comparison of different biomolecular CRISPR/Cas9 formats: Cas9 plasmid, Cas9 mRNA and sgRNA, and Cas9/sgRNA ribonucleoprotein.



although there are a few examples that use polymers or nanoparticles for delivery of two or all three formats.<sup>120–123</sup> Therefore, it is crucial for researchers to know the developed strategies for each format and which problems still remain. Given the different physicochemical and physiological features of Cas9 pDNA, mRNA and RNP, the materials and optimal ratio of each component in certain formulations will differ. In the following sections, the non-viral delivery systems of different CRISPR/Cas9 formats are discussed in detail, and specific examples of each class as well as its reachable target organs specified. In addition, a comprehensive overview over the different biomolecular formats and delivery strategies are provided in Table S1† (pDNA), Table S2† (RNA) and Table S3† (RNP).

### Delivery systems of Cas9 pDNA

**Polymeric delivery systems.** Polyethylenimine (PEI), as a traditional gold standard for pDNA transfections, was also widely used for Cas9 plasmid delivery. For example, Ryu *et al.* developed a 26 kDa branched PEI (BPEI-25K)-based approach for Cas9 plasmid delivery. They found that BPEI-25K could efficiently deliver Cas9 pDNA into Neuro2a cells and induced indels at the Slc26a4 target site.<sup>124</sup> However, such a high-molecular-weight PEI usually exhibits high cytotoxicity, especially at higher dose, which limits its application.<sup>125</sup> To solve this, Zhang *et al.* used  $\beta$ -cyclodextrin ( $\beta$ -CD) to assemble low-molecular-weight PEI (600 Da) into PEI- $\beta$ -CD (PC) as vector for the delivery of Cas9 pDNA. The study showed that PC condensed Cas9 pDNA at high N/P ratios and achieved 19.1% and 7.0% editing efficiencies at the hemoglobin subunit beta and the rhomboid 5 homolog 1 locus, respectively.<sup>126</sup> In another work, Liang *et al.* used a PEG-PEI-Cholesterol (PPC), a lipopolymer which already demonstrated excellent safety in a phase II trial, to encapsulate pDNA encoding vascular endothelial growth factor A (VEGFA) sgRNA and Cas9.<sup>127</sup> To facilitate tumor-specific delivery, they further conjugated an osteosarcoma (OS) cell-specific aptamer LC09 to the lipopolymer. They found that LC09-functionalized PPC achieved selective distribution to both orthotopic OS and lung metastasis, which led to effective VEGFA genome editing and growth inhibition in both cancer models. Recently, a PEI-based multifunctional nucleus-targeting “core-shell” artificial virus (RRPHC) was established by Li *et al.* to knockout the expression of the MutT Homolog1 (MTH1) in ovarian cancer cells.<sup>128</sup> The RRPHC system was composed of a core of fluorinated PEI (1.8K)/Cas9-hMTH1 nanoparticles and a multifunctional shell containing RGD peptide, octa-arginine, PEG and hyaluronic acid (RGD-R8-PEG-HA). The negatively charged HA backbone did not only reduce unspecific interactions in a physiological environment but also achieved CD44 receptor targeting. Moreover, the RGD-R8 peptide provided integrin  $\alpha\beta$ 3 receptor targeting and cell penetration capability to the delivery system. *In vitro* transfection results showed that the MTH1 gene disruption efficiency of RRPHC/Cas9-hMTH1 was better than that of lipofectamine 3000. Moreover, the RRPHC/Cas9-hMTH1 also achieved targeted knockout of MTH1 and significant inhibition of tumor growth *in vivo*.

In other approaches, low-molecular-weight PEI was used as cationic block to modify semiconducting polymers (SPs) for Cas9 pDNA delivery.<sup>129</sup> Li *et al.* fabricated brush-structured SPs (SPPF) by sequentially modifying the backbone of initial SPs using alkyl side chains, PEG chains, and fluorinated PEI (PF).<sup>129</sup> In addition, dexamethasone (Dex), a glucocorticoid that is reported to dilate nuclear pores, was incorporated in the SPPF nanoparticles (SPPF-Dex NPs) to enhance the nuclear entry of Cas9 pDNA. The generated nanoparticles enabled NIR-II imaging guided and NIR-light-triggered genome editing: after administration, the *in vivo* distribution of SPPF-Dex NPs was monitored in real-time by NIR-II imaging and under laser irradiation, the photo-thermal conversion of SPPF promoted the release of Cas9 pDNA from endolysosomes as well as Dex from the NPs. Lyu *et al.* adopted a similar strategy to construct a photolabile SP systems for NIR regulation of gene editing in a HDR model.<sup>130</sup> In this study, PEI600 was conjugated to an  $^1\text{O}_2$ -generating backbone *via*  $^1\text{O}_2$ -cleavable linkers. Upon NIR irradiation, PEI600 was cleaved from the SP backbone, resulting in the release of Cas9 plasmid and subsequent HDR-mediated GFP gene repair. The results showed 15- and 1.8-fold enhancements of GFP expression *in vitro* and *in vivo*, respectively.

In recent years, the FDA-approved polymer poly(lactic-co-glycolic acid) (PLGA) was frequently used for diverse drug delivery applications including nucleic acid delivery.<sup>131,132</sup> Based on the success of cationic lipid-assisted PEG-*b*-PLGA nanoparticles (CLANs) for systemic siRNA delivery, Wang and colleagues developed a series of CLANs for cell type-specific delivery of Cas9 plasmids.<sup>133–137</sup> For example, they encapsulated human CD68 promoter-containing Cas9 plasmids pM330 and pM458 into cationic BHEM-Chol lipid-assisted PEG5K-PLGA11K nanoparticles through a double emulsion method.<sup>136</sup> The obtained CLANpM330 and CLANpM458 were efficiently taken up by T cells, B cells, neutrophils, monocytes and macrophages, but only expressed Cas9 protein in monocytes and macrophages due to the specific human CD68 promoter. Moreover, the functional system CLANpM330/sgNtn1 and CLANpM458/sgNtn1 induced Ntn1 deletion in monocytes and macrophages *in vivo* after intravenous injection. Interestingly, the target cell types of CLANs can be modulated by adjusting the mass fraction of PEG-PLGA and the ratio of the cationic lipid BHEM-Chol.<sup>137</sup> A library of CLANs with various surface PEG densities and surface charges was established and a neutrophils targeting CLAN with lower PEG density and a higher surface charge was identified after screening in high-fat diet (HFD)-induced type 2 diabetes (T2D) mice. The optimized CLAN was able to deliver Cas9 pDNA to the neutrophils of the T2D mice and achieved disruption of the neutrophil elastase (NE) gene both in the liver and white adipose tissue, resulting in an improved glucose tolerance and insulin sensitivity. Besides, CLANs targeting B cells, chronic myeloid leukemia (CML) cells or dendritic cells (DCs) were generated.<sup>133–135</sup> Yang *et al.* prepared lipid-polymer hybrid nanoparticles (LPHNs-cRGD) loaded with a plasmid pCas9/MGMT, targeting O6-methylguanine-DNA methyltransferase,

based on lecithin, DSPE-PEG-cRGD, DSPE-PEG-biotin, PLGA and a nanoprecipitation method.<sup>138</sup> The LPHNs were associated with microbubbles (MBs) composed of DPPC, DSPE-PEG-biotin and cholesterol *via* biotin–avidin interaction. Focused ultrasound (FUS) locally opened the BBB to facilitate the delivery of pCas9/MGMT into the brain *in vivo*, knockout MGMT in glioblastoma and to increase chemosensitivity towards temozolomide (TMZ) therapy. Alternatively to the use of lipids, coating of PLGA nanoparticles with chitosan (CS-PLGA NPs) was also reported.<sup>139</sup> *In vitro* knockout evaluation in HEK293T-GFP cells showed suppression of GFP expression up to 80% by CS-PLGA NPs.

To overcome the general toxicities of conventional transfection reagents, biodegradable polycations, such as poly( $\beta$ -amino ester)s (PBAEs), were generated and used as gene delivery vehicles.<sup>140,141</sup> Deng *et al.* designed a (1-(3-aminopropyl)-4-methylpiperazine) (AMP) modified PBAE (aPBAE) for delivering the CRISPR/Cas9 system to malignant tissues and knocking out cyclin-dependent kinase 5 (Cdk5) *in vivo*.<sup>142</sup> In melanoma and breast cancer models, aPBAE/Cas9-Cdk5 significantly suppressed tumor growth and inhibited lung metastasis after intratumoral injection. To achieve higher transfection efficiency of aPBAE, Gao *et al.* utilized generation 0 PAMAM dendrimers (PAMAM-G0) as a branching unit of PAMAM-PBAE hyperbranched copolymers (hPPC) for Cas9 plasmid delivery.<sup>143</sup> The study showed that hPPC1 with the highest degree

of branching exhibited the strongest plasmid condensation capability and highest transfection efficiency compared with linear PBAE and the moderately branched hPPC2. The Green group synthesized a new class of bioreducible branched ester-amine quadpolymers (rBEAQs) for siRNA and DNA delivery by co-polymerizing acrylate monomers including the disulfide building block 2,2-disulfanediylbis(ethane-2,1-diyl) diacrylate in a one-pot Michael addition reaction.<sup>144</sup> The best formulation of rBEAQs successfully co-delivered Cas9 pDNA and sgRNA into HEK293T-GFP cells and enabled 40% GFP knockout, which was the first time that co-delivery of Cas9 plasmid and sgRNA had been demonstrated for CRISPR-mediated genome editing. More recently, the same group designed a reporter system which enables differentiation between single cleavage edits and deletions mediated by two-fold cleavage edits for evaluating PBAE-based Cas9 pDNA and sgRNA co-delivery systems.<sup>145</sup> The results demonstrated that a decrease of the total DNA dose significantly reduces two-fold cutting events but did not affect the extent of single cut editing.

Recently, it was reported that aminated poly(glycidyl methacrylate) (PGMA) could be a safe and effective gene vector.<sup>146</sup> Zhang *et al.* reported the first example of CRISPR/Cas9-mediated Fbn1 gene editing in the aorta of adult mice using cholesterol (CHO)-terminated ethanolamine-aminated poly(glycidyl methacrylate) (PGEA) (Fig. 7A).<sup>147</sup> The *in vivo* studies showed that the enrichment of the nanosystems in aortic

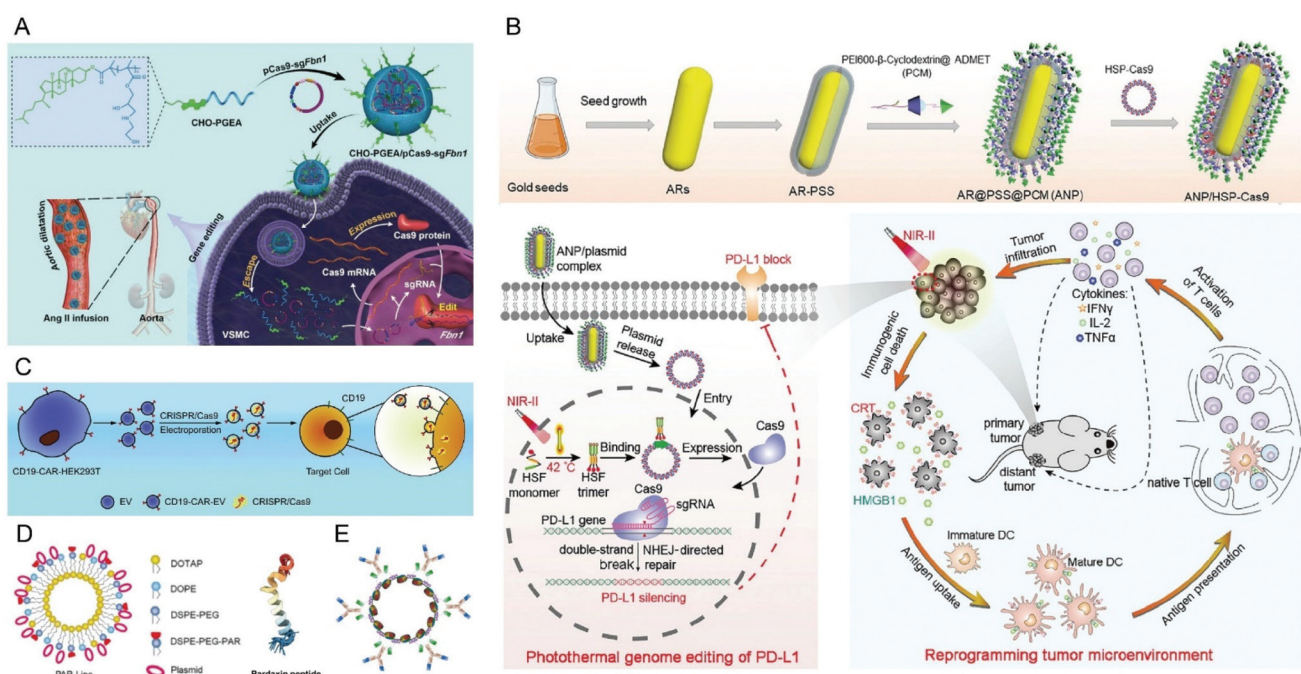


**Fig. 7** Representative delivery systems of Cas9 plasmids. (A) Cholesterol (CHO)-terminated ethanolamine-aminated poly(glycidyl methacrylate) (CHO-PGEA) for gene editing in the aorta. Reproduced with permission from ref. 147. Copyright 2019 John Wiley and Sons. (B) ANP/HSP-Cas9 plasmid complex for a photothermal genome-editing strategy and cancer immunotherapy. Reproduced with permission from ref. 165. Copyright 2021 John Wiley and Sons. (C) Tropism-facilitated delivery of Cas9 plasmids *via* CAR-EVs. Reproduced with permission from ref. 180. Copyright 2020 Elsevier. (D) Delivery of Cas9 plasmids through the non-lysosomal route using pardaxin peptide-modified liposomes. Reproduced with permission from ref. 161. Copyright 2020 John Wiley and Sons. (E) Antibody–chromatin complexes with Cas9 plasmids. Reproduced with permission from ref. 183. Copyright 2019 Oxford University Press.



tissues was improved by Angiotensin II (Ang II) infusion, and efficient *Fbn1* gene disruption was observed in vascular smooth muscle cells (VSMCs) as well as the aorta. Nie *et al.* constructed a responsive charge-reversal carrier (Hep@PGEA/pCas9) which was composed of a negatively charged heparin core and a positively charged cyclodextrin-conjugated PGEA (CD-PGEA) shell to deliver Cas9 plasmids targeting the oncogene survivin for hepatocellular carcinoma therapy.<sup>148</sup> In the reductive milieu of HCC cells with high glutathion concentration, the disulfide cross-linked heparin core disassembled to promote the release of Cas9 pDNA and mediate anti-tumor effects in an orthotopic HCC model. Moreover, the system further improved the therapeutic outcome of sorafenib, providing potential for a combination therapy of HCC.

Apart from synthetic polymers, the natural cationic polysaccharide chitosan has a long tradition as transfecting agent and is still used for the creation of novel gene delivery systems.<sup>149</sup> Recently, a chitosan-based stimuli responsive gene and drug co-delivery system was developed for HCC therapy.<sup>150</sup> In this system, paclitaxel (PTX) and sgVEGFR2/Cas9 plasmid-pre-loaded chitosan was modified with  $\beta$ -galactose-carrying lactobionic acid (LA) to achieve asialoglycoprotein receptor (ASGPR) targeted delivery to HCC cells. *In vivo* knockout studies demonstrated 33.4% genome editing efficiency in tumor tissues and achieved synergistic therapeutic effects with PTX. To overcome the mucoadhesive properties of chitosan, Zhang *et al.* synthesized a series of PEGylated chitosan co-polymers by conjugating methoxy PEG (mPEG) to chitosan, and the obtained PEGylated chitosan was then evaluated for CRISPR/Cas9 plasmid delivery.<sup>151</sup> An *in vitro* mucus model demonstrated that PEGylation of chitosan could improve the mucus-penetration of the nanocomplexes.

Xu's group developed a series of polycations for Cas9 plasmid delivery *via* a one-pot ring-opening reactions.<sup>152–154</sup> By this strategy, an acid-responsive polycation (ARP) with numerous *ortho* ester linkages and hydroxyl groups was synthesized and subsequently fluorinated to produce ARP-F.<sup>152</sup> The obtained ARP-F compacted the plasmid pCas9-survivin within stable nanoparticles and inhibited tumor growth *in vivo* by disrupting the survivin gene. The combination of the nanosystem with temozolomide demonstrated improved antitumoral effects due to an increased sensitivity towards the anticancer drug. Recently, Wang *et al.* fabricated PEGylated nanoparticles (P-HNPs) based on poly( $\gamma$ -4-((2-(piperidin-1-yl)ethyl)amino-methyl)benzyl-L-glutamate) (PPABLGS) for Cas9 plasmid and sgPlk1 delivery.<sup>155</sup> The P-HNPs exhibited excellent colloidal stability and achieved 35% Plk1 knockout in HeLa tumors, resulting in 66.7% down-regulation of Plk1 protein levels, 71% tumor growth inhibition and 60% higher animal survival rate within 60 days. Self-assembled micelles consisting of quaternary ammonium-terminated poly(propylene oxide) (PPO-NMe<sub>3</sub>) and amphiphilic Pluronic F127 were designed by Lao *et al.* for Cas9 plasmid delivery.<sup>156</sup> The optimized micelle system could efficiently delete the E7 oncogene in HeLa cells, which induced an inhibition of the downstream cancerous activity both *in vitro* and *in vivo*. More recently, Emami *et al.* developed

biocompatible 4-arm polyrotaxane (PRX) nanoparticles and optimized them for genome editing. They found that 4-arm PRX modified with a redox-sensitive disulfide linker could improve intracellular pDNA release. The data also demonstrated that 4-arm PRX equipped with the cell penetrating peptide PipB and a peptide targeting the neural cell adhesion molecule (NCAM) successfully delivered Cas9 plasmids to muscle cells and enabled deletion of the DMD exons 45–55.<sup>157</sup>

**Lipidic delivery systems.** An important class of lipidic delivery systems for Cas9 plasmids are 1,2-dioleoyl-3-trimethylammonium-propane (DOTAP)-based cationic liposomes. One example is the work by Zhang *et al.*, who constructed novel cationic liposomes containing DOTAP, DOPE, DSPE-PEG, chondroitin sulfate and protamine for Cas9/sgPlk1 plasmid delivery.<sup>158</sup> Intratumoral injections of the liposomes in melanoma-bearing mice induced significant downregulation of Plk1 protein levels and 67% suppression of tumor growth. To improve the active tumor targeting efficiency of cationic liposomes, various ligand-conjugated DSPE-PEG lipids were developed and utilized.<sup>159,160</sup> Li *et al.* designed a R8-dGR peptide modified lipid for targeting integrin  $\alpha v \beta 3$  and neuropilin-1 to enhance tumor penetration and cell targeting.<sup>160</sup> Co-encapsulation of the Cas9/sgHIF-1 $\alpha$  plasmid and PTX in the generated liposomes enabled downregulation of HIF-1 $\alpha$  and its downstream molecules VEGF and MMP-9, resulting in enhanced antimetastatic effects and synergistic tumor growth inhibition. In another study, multifunctional liposomes were generated containing a pH-sensitive peptide which changes its conformation in the acidic environment of tumors, an epidermal growth factor receptor (EGFR)-targeting peptide and a NLS-peptide for co-delivery of epirubicin for delivery of a CRISPR-Cas9 plasmid targeting the HuR (ELAVL1) gene.<sup>159</sup> The study indicated that the combination of HuR gene disruption and epirubicin treatment promoted cancer cell death *via* apoptosis, necroptosis and autophagy. Yin *et al.* designed cationic liposomes based on DOTAP, which were modified with a cationic peptide pardaxin (PAR) for circumventing the lysosomal pathway and localizing the liposomal carriers to the endoplasmic reticulum (ER) after cellular internalization (Fig. 7D).<sup>161</sup> The results demonstrated that PAR modification avoided the entrapment of cationic liposomes in lysosomes and facilitated the nuclear entry of Cas9 plasmids, which altogether resulted in efficient CDC6 gene disruption and tumor growth inhibition *in vivo*. Alternatively, to cationic liposomes, Li *et al.* reported LNPs (iLP181) based on an ionizable lipid iLY1809 for Cas9 plasmid and sgPlk1 delivery. After a single intravenous injection, iLP181 accumulated and maintained at tumor sites for more than 5 days and achieved distinct tumor growth suppression *in vivo*.<sup>162</sup> Besides, several lipoplex delivery systems for Cas9 plasmid delivery based on pH-sensitive amino lipids have been generated.<sup>163</sup>

**Inorganic and inorganic/organic hybrid delivery systems.** Recently, a series of nanoplatforms based on cationic polymer-coated gold nanorods (AuNR) were developed for Cas9 plasmid delivery by Ping's group.<sup>164–166</sup> For example, they synthesized AuNRs with different aspect ratios (ARs) and assembled them



with poly(sodium-*p*-styrenesulfonate) (PSS) and PEI 25K *via* a layer-by-layer method to encapsulate Cas9 plasmids. The constructed nanorods with a high AR enabled efficient Cas9-mediated gene editing and dCas9-mediated transcriptional activation. *In vivo* studies showed that the delivery approach enabled disruption of the Fas gene and protected mice from liver fibrosis.<sup>164</sup> In other studies, they used Cas9 plasmids with heat-inducible promoter (HSP) in the systems, to realize triggered genome editing by a photothermal effect in the second near-infrared optical window (NIR-II) (Fig. 7B).<sup>165</sup> Besides, Tao *et al.* reported that protamine-functionalized gold nanoclusters could also efficiently complex Cas9 plasmids and deliver them into target cells for genome editing.<sup>167</sup> Silica nanoparticles are developed for diverse delivery applications, including Cas9 plasmids but also the other biomolecular CRISPR/Cas formats. Xu *et al.* constructed poly(dimethyl-diallylammonium chloride) (PDDA)-coated and NLS-modified mesoporous silica nanoparticles (MSNs) for the co-delivery of Cas9 plasmids together with an EGFP DNA template for HDR.<sup>168</sup> The results indicated that the GFP-tag was successfully inserted at the desired locus. Likewise, Zhang *et al.* constructed PAMAM and aptamer coated MSNs for the co-delivery of a Cas9 plasmid and sorafenib.<sup>169</sup> The nanocomplexes exhibited >60% editing efficiency addressing the epidermal growth factor receptor and showed synergistic therapy effects in a tumor-bearing mouse model. Apart from gold and silica nanoparticles, iron oxide nanoparticles were used for Cas9 plasmid delivery.<sup>170</sup> Shen *et al.* constructed MRI-traceable nano-biohybrid complexes based on superparamagnetic iron oxide nanoparticles (SPIONs) which were grafted with dopamine-polylysine-PEG-fluavastatin (DOPA-PLys-PEG-Flu) and dopamine-polylysine-PEG-RVG peptide (DOPA-PLys-PEG-RVG).<sup>170</sup> The generated carriers efficiently delivered fluvastatin and Cas9 plasmids to the brain *via* RVG-facilitated blood–brain barrier crossing, resulting in BACE1 gene disruption with synergistic therapeutic effects in an Alzheimer's disease model. Poddar and co-workers used metal-organic frameworks (MOFs) for Cas9 pDNA delivery. They encapsulated Cas9 plasmids in a zeolitic imidazolate framework ZIF-C composed of Zn<sup>2+</sup> and 2-methylimidazole, which was subsequently coated with epigallocatechin-gallate (EGCG). It was shown that Cas9 plasmid-loaded ZIF-C enabled 20% knockout of the RPSA gene in prostate cancer PC-3 cells, which increased to 25% in case of EGCG-coated particles.<sup>171</sup> Karimi and colleagues generated a series of carbon dots (CDs) based on citric acid and PEI *via* microwave-aided pyrolysis. Vitamin D3-functionalized CDs with low-molecular-weight PEI and fluorescent nitrogen-/zinc-doped CDs with PEI 25K demonstrated effective GFP gene disruption.<sup>172,173</sup> Recently, a light-activated charge-reversal pCas9 nanovector (UCNP-UVP-P) was fabricated by coating upconverting nanoparticles with a light-sensitive polyelectrolyte.<sup>174</sup> Under 980 nm light irradiation, cationic residues of the polyelectrolytes detached, which converted the positively charged nanovectors into negatively charged particles, and induced Cas9 plasmid release. *In vivo* antitumor studies showed that UCNPs-UVP-P achieved approximately 42.5% Plk1 gene

knockout and effectively inhibited tumor growth under photo-irradiation. Cheng and colleagues developed various CaCO<sub>3</sub>-based delivery systems for Cas9 plasmid delivery.<sup>175–177</sup> One example is a multifunctional nanovector, containing the CRISPR-Cas9 plasmid, CaCO<sub>3</sub> and protamine sulfate (PS) in the core which is coated with AS1411 aptamer-conjugated hyaluronic acid (AHA) and TAT-NLS peptide-conjugated hyaluronic acid (PHA). The vector could induce robust β-catenin knockout and suppressed the Wnt/β-catenin pathway, which also resulted in inhibition of PD-L1-mediated immunosuppression.<sup>175</sup>

**Bio-derived vesicles.** Bio-derived vesicles have drawn interest in drug and gene delivery research due to their low immunogenicity, high cellular uptake and excellent loading capacity for various cargos.<sup>178</sup> Recently, Kim *et al.* developed tumor-derived exosomes for Cas9 plasmid delivery.<sup>179</sup> They found that tumor-derived exosomes outperformed epithelial cell-derived exosomes *in vivo* due to their cell tropism. Loaded with a CRISPR-Cas9 plasmid targeting poly(ADP-ribose) polymerase-1 (PARP-1), the tumor-derived exosomes achieved efficient suppression of PARP-1, which induced apoptosis in ovarian cancers and enhanced the chemo-sensitivity towards cisplatin. Instead of cancer-derived extracellular vesicles (EVs), Xu *et al.* used epithelial cell-derived vesicles that were further modified with a chimeric-antigen receptor (CAR) to enable a tropism-facilitated delivery (Fig. 7C).<sup>180</sup> CAR-EVs exhibited faster accumulation in tumors than normal EVs and effectively disrupted MYC oncogene both *in vitro* and *in vivo*. To further improve the efficiency of exosomes to encapsulate large sized nucleic acids such as Cas9 plasmids, Lin *et al.* generated exosome-liposome hybrid nanoparticles.<sup>181</sup> The hybrid systems could efficiently encapsulate Cas9 plasmids and induced gene editing in mesenchymal stem cells (MSCs).

**Protein-based.** As discussed above, Cheng's group generated a series of CaCO<sub>3</sub>-based delivery systems for CRISPR-Cas9 plasmids. Alternatively to the CaCO<sub>3</sub> core, they assembled histones and KALA peptides with Cas9 plasmids *via* electrostatic interactions, and subsequently modified the core with HA and AS1411-HA to achieve targeted delivery with the final vectors.<sup>182</sup> The constructed nanoparticles realized potent PPM1D gene editing with significantly reduced PPM1D expression, which resulted in the reversal of tumor malignancy. Likewise, Killian *et al.* reported targeted chromatin that was assembled from CRISPR-Cas9 plasmids and histones and subsequently modified with bi-specific antibody derivatives (bsAbs). The delivery system exhibited high cellular uptake efficiency due to antibody-mediated cell binding and thereby enabled efficient genome editing in MCF7 cells (Fig. 7E).<sup>183</sup> In addition to histones, human serum albumin nanoparticles with pDNA/stearyl-PEI core were recently reported for Cas9 plasmid delivery as well.<sup>184</sup>

#### Delivery systems of Cas9 mRNA and sgRNA

**Polymeric delivery systems.** As discussed in the section above, a series of cell type-specific CLANs were developed for CRISPR-Cas9 plasmid delivery. The same group also reported CLANs for the encapsulation and delivery of Cas9 mRNA and a



sgRNA targeting the costimulatory molecule CD40.<sup>185</sup> The CLANS effectively delivered Cas9 mRNA/sgCD40 into dendritic cells and disrupted CD40 both *in vitro* and *in vivo*. In an acute mouse skin transplant model, CLAN-mediated CD40 knockout markedly inhibited T cell activation, resulting in reduction of graft damage and prolongation of graft survival. Li *et al.* reported other PLGA-based nanoparticles for Cas9 mRNA/sgRNA delivery.<sup>186</sup> Specifically, they used a microfluidic chip to coat a PLGA core with cationic lipids to form positively charged nanoparticles capable of binding negatively charged Cas9 mRNA and sgRNA. The developed nanosystem increased gene editing efficiency by 3-fold compared to commercially available non-viral carriers. Kataoka and co-workers prepared Cas9 mRNA/sgRNA polyplex micelles (PMs) using a block-copolymer of polyethylene glycol and a poly(aspartamide) with the short oligoamine diethylene triamine (DET) in the side chain (PEG-PAsp(DET)) for genome editing in the brain (Fig. 8A).<sup>187</sup> The study showed that co-loading of Cas9 mRNA and sgRNA into single PMs had better stability than loading of sgRNA alone. After intraparenchymal injection, PMs with co-encapsulated RNA widely induced genome editing in parenchymal cells, including neurons, astrocytes, and microglia. Utilizing the noncoding poly(A) tail of the mRNA, Huang *et al.* constructed PEI-coated and DNA-linked poly(T20)-grafted polycaprolactone (T20-g-PCL) nanogels for Cas9 mRNA delivery.<sup>188</sup> The PEI-coated nanogels demonstrated robust eGFP knockout in a sgEGFP expressing 293T-EGFP cell model.

**Lipidic delivery systems.** Lipid nanoparticles (LNPs) are the most-used and most successful lipidic delivery system for Cas9 mRNA and sgRNA. Yin *et al.* first reported the success of Cas9 mRNA delivery into the liver using C12-200 lipid nanoparticles (LNPs).<sup>189</sup> Together with adeno-associated viruses carrying the genetic information for a sgRNA targeting Fah<sup>mut/mut</sup> and a HDR template, the combined viral and LNP delivery system achieved Fah correction in more than 6% of hepatocytes after a single treatment. Considering several limitations of viral vectors, Dong and co-workers reported the first example of non-viral delivery of Cas9 mRNA and sgRNA to the mouse livers by TT3 lipid-like nanoparticles (LLN).<sup>190</sup> *In vivo* studies demonstrated that one injection of Cas9 mRNA LLNs followed by an injection of sgRNA LLNs 6 h later caused a remarkable reduction of PCSK9 protein levels in mice. Instead of two injections, Finn *et al.* developed an LNP-based delivery system, called LNP-INT01, that allowed co-encapsulation of Cas9 mRNA and sgRNA into the same particles for simultaneous delivery with a single dose.<sup>71</sup> After intravenous injection, LNP-INT01 enabled significant editing of the mouse transthyretin (TTR) gene in the livers, achieving >97% reduction of serum protein levels that persisted for over 12 months. Recently, Xu's group designed a series of bioreducible lipidoids for Cas9 mRNA/sgRNA delivery.<sup>191–194</sup> For example, BAMEA-O16B, one of the leading lipids, formulated with the helper lipids, DSPE-PEG2000 and Cas9 mRNA/sgPCSK9 could reduce PCSK9 protein levels in mouse serum to

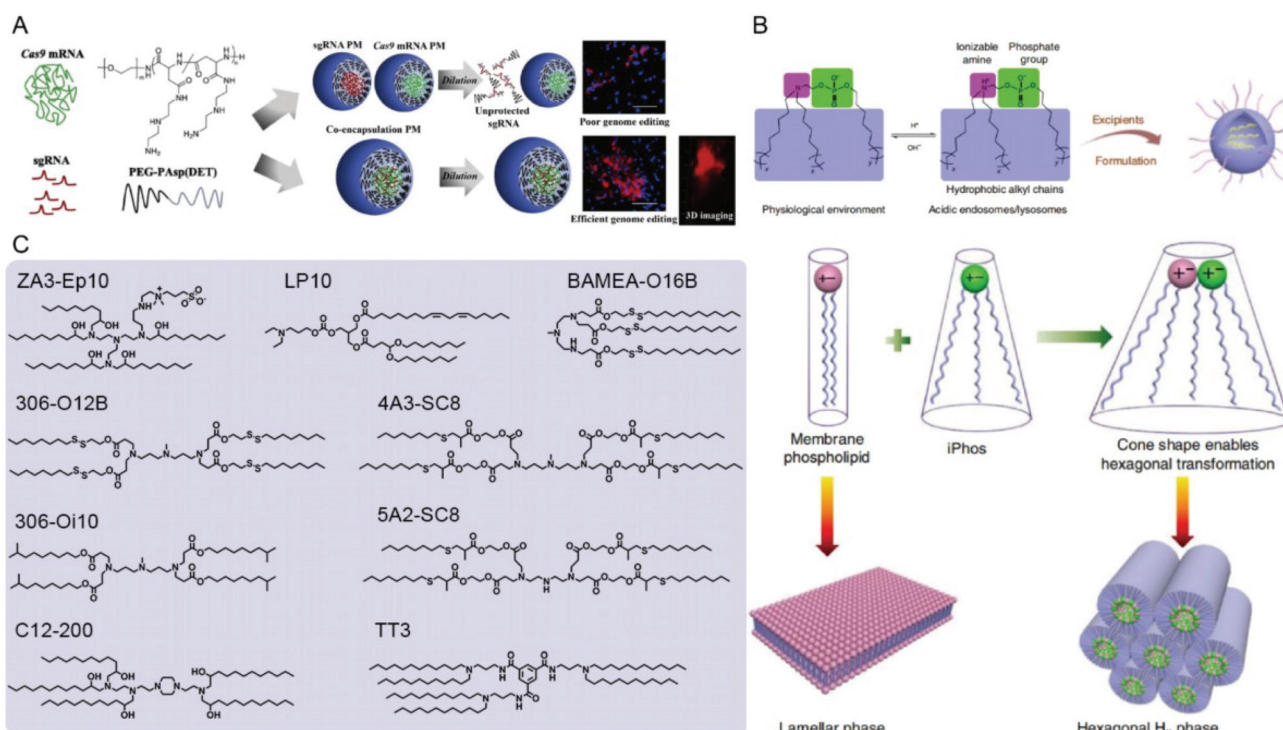


**Fig. 8** Representative delivery systems of Cas9 mRNA and sgRNA. (A) Poly(aspartamide)-based Cas9 mRNA/sgRNA polyplex micelles (PMs) for genome editing in the mouse brain. Reproduced with permission from ref. 187. Copyright 2021 Elsevier. (B) Multi-tailed ionizable phospholipids (iPhos) with enhanced hexagonal transformation capability at endosomal pH. Reproduced with permission from ref. 197. Copyright 2021 Springer Nature. (C) Representative lipids used for Cas9 mRNA and sgRNA delivery.



20%.<sup>191</sup> Using another highly potent tail-branched bioreducible lipidoid 306-O12B, the constructed LNPs successfully delivered Cas9 mRNA and sgRNA against Angiopoietin-like 3 (Angptl3) to the mouse liver hepatocytes, inducing 38.5% editing events and 65.2% reduction of serum Angptl3 protein levels.<sup>193</sup> The editing effect was maintained at a therapeutic relevant level for at least 100 days after one single dose. The same group also reported a new class of cholesteryl-based bioreducible lipidoids as well as another type that showed effective Cas9 mRNA delivery to human mesenchymal stem cells (hMSCs).<sup>192,194</sup> As an alternative to disulfide bond-containing bioreducible lipids, Zhang *et al.* designed a series of lipid-like compounds containing ester groups for Cas9 mRNA delivery.<sup>195</sup> The study showed that linear ester chains were degraded much faster than branched ester chains and both types demonstrated efficient Cas9 mRNA delivery *in vitro* and *in vivo*. Being different from classic ionizable lipids, Siegwart and colleagues developed a new class of zwitterionic amino lipids (ZALs) that contain a zwitterionic sulfobetaine head group for Cas9 mRNA and sgRNA delivery.<sup>46</sup> ZAL nanoparticles enabled high protein expression at low doses *in vitro* (<600 pM) and *in vivo* (1 mg kg<sup>-1</sup>). After intravenous administration, genome editing events were observed in the liver, kidneys and lung. Currently, the liver is a main target organ of systemic LNP administrations, although some other tissues are also reached. Rational design of nanoparticles for a controlled and predictable delivery to different organs is still a big challenge. Recently, Siegwart's group reported selective organ targeting (SORT) LNPs which are supplemented with SORT molecules, such as DODAP, DOTAP or 1,2-dioleoyl-*sn*-glycero-3-phosphate (18-PA), that allow systematic engineering of nanoparticles for delivery of various cargos including mRNA, Cas9 mRNA/sgRNA and Cas9 RNPs to the lungs, spleens and livers.<sup>196</sup> In a *tdTomato* reporter mouse model, significant *tdTomato* fluorescence recovery was achieved in the livers with mDLNP as well as 20% DODAP SORT LNPs, in the lungs with 50% DOTAP SORT LNPs and in the spleen with 30% 18PA SORT LNPs. Moreover, the SORT LNPs were also able to edit endogenous PTEN and PCSK9 genes. For instance, 20% DODAP SORT LNPs mediated around 60% indels at the PCSK9 site which led to approximately 100% reduction of PCSK9 liver and serum protein levels. Inspired by natural phospholipids, they further developed multi-tailed ionizable phospholipids (iPhos) with enhanced membrane hexagonal transformation capability for Cas9 mRNA/sgRNA delivery (Fig. 8B).<sup>197</sup> iPhos together with helper lipids formed multi-component lipid nanoparticles (iLNPs), enabling tissue-selective CRISPR-Cas9 gene editing. Recently, dendrimer-based LNPs (dLNPs) that co-encapsulated Cas9 mRNA, sgRNA and donor DNA for HDR repair in xenograft tumors *in vivo* was reported by the same group.<sup>198</sup>

In addition to SORT LNPs, other cell-selective or targeted LNPs were generated for specific applications. For instance, Peer and colleagues modified LNPs by coating them with anti-hEGFR to target human serous ovarian adenocarcinomas Ovar8 (OV8) that highly express EGFR.<sup>199</sup> Intraperitoneal injections of EGFR-targeted sgPlk1-LNPs into mice with disse-

minated peritoneal OV8 tumors achieved up to ~80% gene editing *in vivo*, resulted in tumor growth inhibition and increase of survival by 80%. Tang *et al.* designed sialic acid-targeted phenylboronic acid (PBA)-derived LNPs which achieved much higher knockouts in HeLa cells than in non-cancer cells.<sup>200</sup>

The high potential of LNPs for RNA delivery in humans is not only demonstrated by the extensively used mRNA COVID-19 vaccines, but also the first clinical trial of systemic CRISPR-Cas9 *in vivo* gene editing, which is based on Cas9 mRNA and sgRNA.<sup>119</sup> Gillmore *et al.* recently published interim results of the phase 1 clinical study. Six patients suffering from hereditary transthyretin amyloidosis (ATTR) were treated with a CRISPR LNP formulation targeting the transthyretin (TTR) gene to reduce the concentration of misfolded protein in serum. Single administrations resulted in 52% mean reduction of TTR serum levels at a dose of 0.1 mg kg<sup>-1</sup> and 87% reduction at 0.3 mg kg<sup>-1</sup>. In a safety assessment period within 28 days after infusion only few and mild adverse reactions were observed. The study can be considered a milestone in the development of *in vivo* genome editing therapeutics and presumably is just the beginning of numerous developments in the future.

## Delivery systems of Cas9 RNPs

**Polymeric delivery systems.** Similar to the delivery of CRISPR-Cas9 plasmids, PEI as a cationic unit with favourable properties for cellular transport of biomolecules is also widely used for Cas9 RNP delivery. For example, core-shell liposome-templated hydrogel nanoparticles (LHNPs) were developed by crosslinking cyclodextrin (CD)-engrafted PEI (25K) (PEI-CD) with adamantine (AD)-engrafted PEI (25K) (PEI-AD) through CD-AD host-guest interactions and subsequent DOTAP liposome coating.<sup>201</sup> The study indicated that LHNPs carrying Cas9/sgPlk1 effectively inhibited tumor growth and prolonged the survival time of tumor-bearing mice. The concept of constructing supramolecular nanoparticles *via* CD-AD mediated host-guest interaction was also validated in other systems for Cas9 RNP delivery.<sup>202–204</sup> Wan *et al.* complexed disulfide-bridged guanidyl AD (AD-SS-GD) with β-CD-conjugated low-molecular-weight PEI (CP) to generate CP/AD-SS-GD for loading Cas9 RNPs.<sup>202</sup> CP/AD-SS-GD/RNP exhibited efficient cellular uptake and could readily release Cas9 RNPs in the reductive intracellular environment. They further found that hyaluronic acid coated CP/AD-SS-GD/RNP targeting mutant KRAS could effectively suppress tumor growth and metastasis *in vivo*. In another work, the CP/AD-SS-GD/RNP targeting NLRP3 were packaged together with dexamethasone-loaded polymeric nanoparticles into a dissolvable microneedle (MN) patch. The transdermal co-delivery achieved synergistic therapeutic effects against inflammatory skin disorders in mouse models.<sup>203</sup> Ban *et al.* prepared Cas9 RNP-loaded supramolecular nanoparticles (RNP-SMNPs) *via* mixing AD-PAMAM, AD-PEG, AD-PEG-TAT, CD-PEI and Cas9 RNPs. The optimized RNP-SMNPs enabled specific deletion of the dystrophin exons

45–55 as a potential approach for the treatment of Duchenne muscular dystrophy.<sup>204</sup>

In addition to PEI, cationic polypeptides such as polylysine and poly(aspartic acid) with cationic side-chain modifications were developed which generally feature higher biocompatibility and lower toxicity.<sup>205,206</sup> Liu *et al.* reported a nano-Cas9 RNP system (nanoRNP) based on 2,5-dihydro-2,5-dioxofuran-3-acetic acid (CA)-bridged polylysine-g-poly(ethylene glycol) (PLys100-CA-mPEG77).<sup>205</sup> The nanoRNP detached its mPEG shell in the acidic tumor microenvironment, facilitated cellular uptake of Cas9 and a combination of sgRNAs targeting STAT3 and RUNX1, which resulted in effective tumor growth inhibition in a heterogenous tumor model. Deng *et al.* utilized two copolymers to construct a tumor-targeted gene editing system for synergistic gene and photodynamic antitumoral effects (Fig. 9A).<sup>206</sup> Firstly, nitrilotriacetic acid-disulfanediylpropionate-polyethyleneglycol-*b*-polycaprolactone (NTA-SS-PEG-PCL) was assembled with the hydrophobic photosensitizer chlorin e6 (Ce6) into a micellar core. Then the chelate complexes of NTA with nickel ions on the surface of the micelles bound oligohistidine-tag containing Cas9 RNPs *via* coordinative interactions. Finally, iRGD-PEG-*b*-polyasparte-*g*-1,4-butanediamine [RGD-PEG-pAsp(DAB)] was added to neutralize the negative charge of the NPs and to provide tumor-targeting ability. The obtained T-CC-NPs escaped from lysosomes *via* NIR-induced production of reactive oxygen species (ROS) by Ce6 and released their Cas9/sgNrf2 cargo due to the reduction of disulfide bonds. The study indicated that Nrf2 deletion

enhanced tumor cell sensitivity to ROS, leading to synergistic effects of PDT and Nrf2 gene knockout *in vivo*.

As discussed in the previous pDNA part, PBAEs have been utilized as vectors for CRISPR-Cas9 plasmid delivery. In the context of protein delivery, classical PBAEs with highly positive charge may not be appropriate to encapsulate Cas9 proteins due to incompatibility with the surface charge density. Therefore, Green *et al.* synthesized a new class of PBAEs which contain both cationic and anionic functions *via* polymer end-capping with carboxylate ligands.<sup>207</sup> The carboxylated PBAEs could self-assemble into nanoparticles with various types of proteins including Cas9 RNPs. The study demonstrated that a single intracranial injection of the nanoparticles carrying 3.5 pmol Cas9 RNP induced robust gene editing in an orthotopic murine glioma model. Likewise, Chen *et al.* synthesized a glutathione (GSH)-cleavable cross-linked polymer containing both cationic and anionic residues for better encapsulation of inhomogeneously charged Cas9 RNPs.<sup>208</sup> After local administration *in vivo*, the optimized nanoparticles enabled robust gene editing in retinal pigment epithelium (RPE) tissues and skeletal muscles. Recently, Liu *et al.* reported a phenylboronic acid-modified dendrimer that could also bind both negatively and positively charged proteins.<sup>209</sup> The dendrimer effectively delivered various native proteins with different isoelectric points and sizes into cells. Particularly, it enabled efficient delivery of Cas9 RNPs into multiple cell lines and achieved excellent editing efficiency. Although numerous types of polymers were successfully synthesized and optimized for Cas9

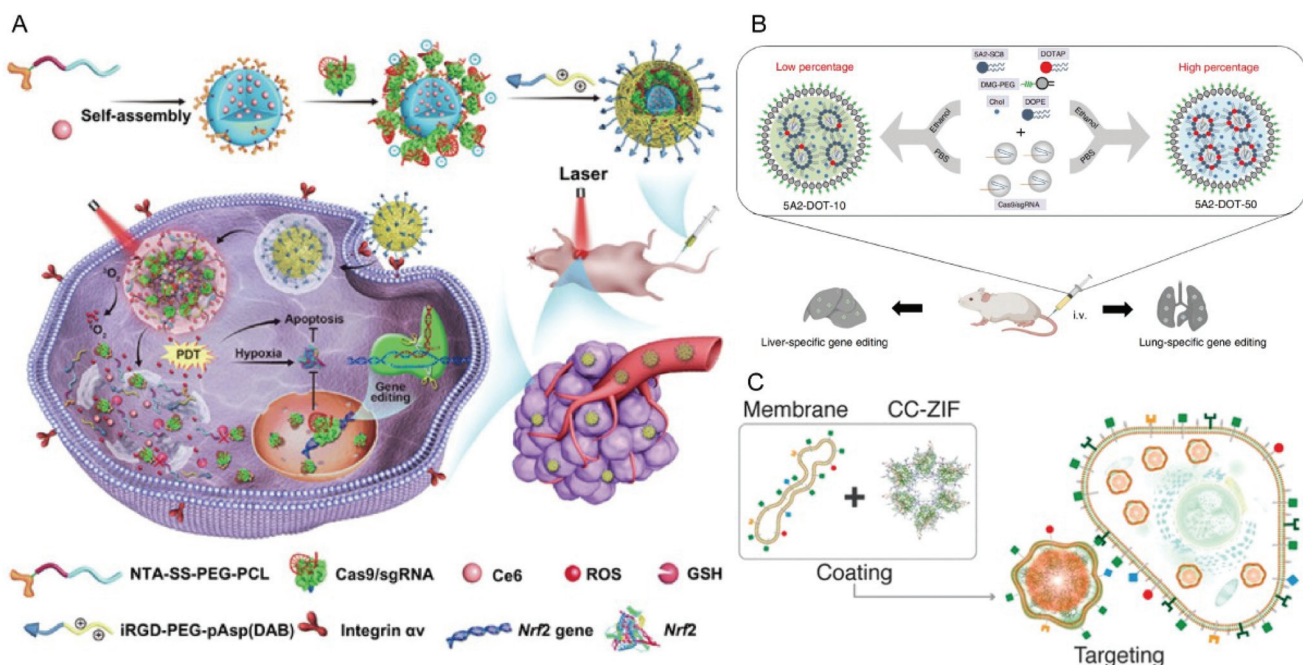


**Fig. 9** Representative delivery systems of Cas9 RNP. (A) Codelivery of Cas9 RNP and chlorin e6 for spatially controlled tumor-specific genome editing *in vivo*. Reproduced with permission from ref. 206. Copyright 2020 American Association for the Advancement of Science. (B) Tissue specific genome editing using DOTAP incorporated lipid nanoparticles. Reproduced with permission from ref. 89. Copyright 2020 Springer Nature. (C) Cell-type-specific Cas9 RNP delivery by cell membrane-coated ZIF-8. Reproduced with permission from ref. 222. Copyright 2020 American Chemical Society.



RNP delivery, the question on structure–activity relationships is still hard to answer. For this purpose, Kumar *et al.* validated that combinatorial synthesis and high-throughput characterization methodologies coupled with machine learning enables the rapid discovery of potential polymers for Cas9 RNP delivery, which may accelerate the clinical translation of polymeric vectors in the future.<sup>210</sup>

**Lipidic delivery systems.** In 2015, Zuris *et al.* first validated that a commercially available cationic lipid reagent (Lipofectamine RNAiMAX) could efficiently deliver engineered highly anionic proteins as well as pre-assembled Cas9/sgRNA RNPs into cells.<sup>44</sup> Particularly for Cas9 RNPs, cationic lipid-mediated delivery achieved up to 80% genome modification *in vitro* and 20% in the mouse inner ear *in vivo*. After the success of common transfection reagents, LNPs which are mostly used for Cas9 mRNA delivery were also optimized for Cas9 RNPs. For example, bioreducible LNPs were loaded with the chemokine CXCL12 $\alpha$  and Cas9 RNPs targeting the interleukin-1 receptor accessory protein (IL1RAP). After the fabrication, the LNPs were loaded onto mesenchymal stem cell membrane-coated nanofibril (MSCM-NF) scaffolds to enhance targeting of leukemia stem cells for the therapy of acute myeloid leukemia (AML).<sup>211</sup> It is worth noting that the common LNP formulation process for nucleic acids is performed in acidic buffer which is not suitable for Cas9 RNPs, due to potential denaturation of the protein and decrease of the final editing efficiency. To circumvent this problem, Wei *et al.* developed a generalizable approach that allows Cas9 RNP encapsulation in neutral buffers by adding a permanently cationic lipid to the conventional LNP formulations (Fig. 9B).<sup>89</sup> By optimizing the lipid components and ratios, the generated LNPs enabled tissue-specific gene editing and multiple genome modifications in mice. Recently, stimuli-triggered liposomes were designed for temporal and spatial control of Cas9 RNP-mediated gene editing.<sup>212,213</sup> Aksoy *et al.* developed light-triggered liposomes by integrating a photosensitive compound, verteporfin (VP), into the lipid bilayer.<sup>212</sup> Upon 690 nm light illumination, singlet oxygen generated by VP destabilized the liposomal structure and facilitated Cas9 RNP release. The temporal and spatial control of gene editing was achieved both *in vitro* and in a zebrafish model. In another study, Ryu *et al.* designed an ultrasound (US)-activated microbubble conjugated nanoliposome (MB-NL) to utilize Cas9 RNPs for the therapy of androgenic alopecia.<sup>213</sup> Under high acoustical wave ultrasound frequency, MB-NL enabled improved Cas9 RNP delivery to dermal papilla cells (DPC), resulting in efficient steroid type II 5-alpha-reductase (SRD5A2) gene knockout and subsequent hair growth recovery.

**Inorganic and inorganic/organic hybrid delivery systems.** Recently, Lee *et al.* developed DNA-thiol modified gold nanoparticles (GNPs) that could firstly hybridize with donor DNA and then absorb Cas9 RNPs onto the surface of GNPs.<sup>214</sup> The Cas9 RNP-loaded GNPs were further coated with a layer of silica for increasing the negative charge density and finally complexed with the cationic polymer PAsp(DET). The obtained CRISPR-gold induced 5.4% correction of the dystrophin gene

in mdx mice and improved animal strength under clinically relevant conditions. Other gold nanoparticles modified with PEI were reported that could not only deliver Cas9 but also the alternative RNA-guided endonuclease Cpf1 (Cas12a) together with the required crRNA and ssDNA template into haematopoietic stem and progenitor cells (HSPCs).<sup>215</sup> Zhang *et al.* constructed a multi-targeting Cas9 RNP delivery systems from gold nanoclusters by conjugation of the cell penetrating HIV-1-transactivator-of-transcription (TAT) peptide and lipid-coating with galactopyranoside (Gal)-modified DOTAP.<sup>216</sup> Encapsulated Cas9 RNPs targeting the PCSK9 gene enabled about 60% PCSK9 knockout *in vitro* and around 30% plasma LDL cholesterol reduction *in vivo*. Interestingly, the recent studies found that the Cas9 RNP corona, which is formed on the surface of AuNPs, could already mediate efficient cellular uptake without requirement of further complexation by polymers or lipids.<sup>217</sup> Utilizing the interactions between carboxylates and guanidinium groups, Rotello and colleagues assembled arginine AuNPs (ArgNPs) with oligo(glutamic acid)-tagged Cas9 protein to generate a series of Cas9En-ArgNP nanoassemblies for direct cytosolic delivery of Cas9 RNPs.<sup>43</sup> The study demonstrated that the delivery efficiency of Cas9En increased with increasing E-tag length from E0 to E20, and up to 90% of the cells were reached when Cas9E20 was used. After systemic injection of Cas9E20-ArgNPs, the efficient gene editing of the PTEN gene was observed, especially in macrophages in the liver and spleens.<sup>218</sup> Apart from spherical gold nanoparticles, nanoparticles with other shapes, such as nanorods (AuNRs) and nanowires (AuNWs), were also utilized.<sup>219,220</sup> For instance, Li *et al.* developed azobenzene-4,4'-dicarboxylic acid (p-AZO) modified AuNRs to achieve hypoxia-responsive on-demand release of Cas9 RNPs for mild-photothermal therapy.<sup>219</sup> Hansen-Bruhn *et al.* constructed an ultrasound-propelled nanomotor based on AuNWs for active and direct intracellular delivery of Cas9 RNPs.<sup>220</sup> The nanomotors achieved efficient knockout with only 0.6 nM of Cas9 protein.

In 2017, zeolitic imidazolate framework-8 (ZIF-8), a subclass of metal-organic frameworks (MOFs), was reported as the first example of MOF-based Cas9 RNP delivery by Khashab and colleagues.<sup>221</sup> The CRISPR/Cas9 ZIF-8 (CC-ZIF) achieved 17% loading efficiency of Cas9 RNPs and 37% EGFP knockout *in vitro*. Moreover, they coated CC-ZIF with cancer cell membranes (C3-ZIF<sub>cell membrane type</sub>) to enable cell-type-specific delivery of Cas9 RNPs (Fig. 9C).<sup>222</sup> *In vitro* studies demonstrated higher repression of EGFP reporter expression when MCF-7 cells where treated with C3-ZIF<sub>MCF-7</sub> compared to C3-ZIF<sub>HeLa</sub>, and in HeLa cells *vice versa*. *In vivo* fluorescence imaging confirmed that C3-ZIF<sub>MCF-7</sub> could specifically accumulate in MCF-7 tumor sites. Recently, Yang *et al.* assembled imidazole-2-carboxaldehyde (2-ICA) and Zn<sup>2+</sup> with Cas9 RNPs to generate an ATP-responsive delivery system (ZIF-90).<sup>223</sup> The intracellular high concentration (10 mM) of ATP disassembled ZIF-90 due to the competitive coordination between Zn<sup>2+</sup> and ATP, released Cas9 RNPs and induced up to 35% GFP knockout in HeLa cells. Liu *et al.* reported a novel approach for controlling hierarchical self-assembly of metal-organic cages

(MOC) into supramolecular nanoparticles (SNPs) for Cas9 RNP delivery.<sup>224</sup> The adamantane-functionalized  $Pd_{12}L_{24}$  MOC (Ada-MOC) and  $\beta$ -cyclodextrin-conjugated PEI (PEI- $\beta$ CD) assembled *via* host-guest interaction and encapsulated Cas9 RNPs. The obtained Cas9 SNPs achieved 40% knockout of GFP expression compared to non-treated cells.

As discussed in previous sections, mesoporous silica nanoparticles (MSNs) are widely used for delivery purposes, including the CRISPR/Cas9 system in nucleic acid or RNP form. However, the common technique of protein loading into MSNs is based on nonspecific physical absorption, which generally results in rather weak binding. To enhance the encapsulation efficiency of the protein in MSNs, Liu *et al.* developed a novel approach by modifying the surface of Cas9 protein with boronic acid and MSN scaffolds with amine groups.<sup>225</sup> The dative bond formation between boronic acids and amines as well as electrostatic interactions increased the loading and intracellular delivery of Cas9 RNPs. Recently, Pan *et al.* constructed NIR-responsive upconversion nanoparticles (UCNPs) for Plk1 gene disruption in tumors.<sup>226</sup> In this system, Cas9 RNPs were covalently anchored on the surface of UCNPs *via* a photocleavable 4-(hydroxymethyl)-3-nitrobenzoic acid (ONA) linker, and the formed UCNPs-Cas9 complexes were coated with PEI to facilitate endosomal escape after cellular internalization. Upon irradiation, UCNPs-Cas9@PEI converted 980 nm NIR light into local ultraviolet light which resulted in photo-responsive release of Cas9 RNPs and significant inhibition of tumor cell growth both *in vitro* and *in vivo*. In another study, Chen *et al.* used semiconducting copper sulfide (CuS) NPs as NIR-absorbing nanomaterials along with Cas9 RNPs, doxorubicin (DOX) and PEI to establish multifunctional NIR-triggered nanocomplexes for cancer combination therapy based on photothermal and chemotherapy.<sup>227</sup> Besides, several 2D-nanomaterials were reported for Cas9 RNP delivery.<sup>228,229</sup> Yue *et al.* developed a PEG and PEI dual-functionalized graphene oxide (GO) platform which enabled Cas9 RNP loading and CRISPR-mediated gene editing.<sup>228</sup> Zhou *et al.* engineered a Cas9 protein with three NLS tags (Cas9N3) at the C terminus for a better loading onto black phosphorus nanosheets (BPs) *via* electrostatic interactions.<sup>229</sup> The constructed Cas9N3-BPs entered the cells *via* both direct membrane penetration and endocytosis pathways, and the Cas9N3 with improved nuclear entry led to robust gene editing *in vitro* and *in vivo*.

**Peptidic delivery systems.** In general, peptide-mediated RNP delivery can be divided into two strategies: (1) covalent linkage of cell-penetrating peptides (CPPs) to the Cas9 protein; and (2) non-covalent assembly of peptides with Cas9 RNPs into nanocomplexes. The first strategy can be further sub-classified into chemical conjugation of CPPs or genetic engineering. Kim and colleagues reported the first example of chemical Cas9 protein delivery based on CPPs in 2014.<sup>230</sup> They conjugated arginine-rich CPPs to Cas9 protein *via* thiol-maleimide reaction and treated cells along with CPP-complexed sgRNA. The results showed that CPP-mediated Cas9 delivery exhibited efficient gene editing in multiple cell lines with reduced off-target effects compared to plasmid transfections. Gao and colleagues

genetically fused a supercharged polypeptide (SCP) to proteins to facilitate direct intracellular transduction without requirement of additional delivery agents.<sup>231</sup> They found that K4-tagged proteins achieved highest cellular uptake and distribution into the nucleus. For genome editing, Cas9-K4/sgRNA induced 15.2% indels in the CCR5 gene in HeLa cells. However, the activity of Cas9 was affected by the modification and the cleavage efficiency of SCP-fused Cas9 decreased, eventually due to steric hindrance. To solve this drawback, they introduced a cleavable dithiocyclopeptide linker between Cas9 and SCP which contains a matrix metalloproteinase 2 (MMP-2) recognition site and an intramolecular disulfide bond (denoted Cas9-linker-SCP).<sup>232</sup> Free Cas9 proteins were sufficiently released from Cas9-linker-SCP *via* extracellular MMP-2 cleavage and subsequent intracellular GSH-induced disulfide break, which resulted in enhanced genome editing efficiency. In another study, Kim *et al.* developed a carrier-free Cas9 RNP delivery strategy by engineering Cas9 protein containing a NLS and a low-molecular-weight protamine (LMWP).<sup>233</sup> The generated Cas9-LMWP self-assembled with crRNA:tracrRNA to form ternary Cas9 RNPs, which were efficiently taken up by cells and enabled KRAS gene disruption *in vitro* and *in vivo*. In addition to covalent conjugates, various types of peptides were synthesized to form nanocomplexes with Cas9 RNPs *via* electrostatic interactions. Park *et al.* reported that amphiphilic R7L10 peptides could form stable complexes with Cas9 RNPs.<sup>234</sup> The obtained complexes were able to knockout Bace1 gene in the mouse brain, resulting in the suppression of amyloid beta (A $\beta$ )-associated pathologies and cognitive deficits in two mouse models of Alzheimer's disease. Krishnamurthy *et al.* rationally designed three shuttle peptides derived from the endosomolytic peptide CM19 and the CPP PTD4 for protein delivery.<sup>235</sup> These shuttle peptides could bind Cas proteins (SpCas9 or AsCas12a) *via* noncovalent interactions and mediated entry into mouse airway epithelial cells, which enabled gene editing of loxP sites in airway epithelia of ROSAmT/mG mice. Lipid-modified peptides (lipopeptides) were widely used for Cas9 RNP delivery as amphiphilic molecules with tunable properties which can assemble into nanomicelles and have favourable interaction potential with cellular membranes. For example, Thach *et al.* synthesized lipopeptides derived from a blood-brain barrier permeable peptide dNP2 which was modified with different saturated fatty acids (C8:0, C10:0, C14:0) for the delivery of 'hyperaccurate' Cas9 RNPs (HypaRNP) (Fig. 10A).<sup>236</sup> The dNP2 lipopeptides allowed efficient intracellular delivery of HypaRNPs, resulting in up to 26.7% and 19.7% genome modifications in human embryonic kidney and glioblastoma cells, respectively. Likewise, Jain *et al.* designed a tandem peptide that consists of a targeting peptide, a CPP and a lipid tail.<sup>237</sup> By structural optimization, the created tandem peptides successfully delivered Cas9 RNPs in multiple cell lines and achieved robust gene editing. Kuhn *et al.* developed a library of sequence-defined oligo(ethylenamino) amides, a type of artificial peptides, which are based on the oligoamino acid succinoyl-tetraethylene-pentamine (Stp). The oligomers with T-shape archi-



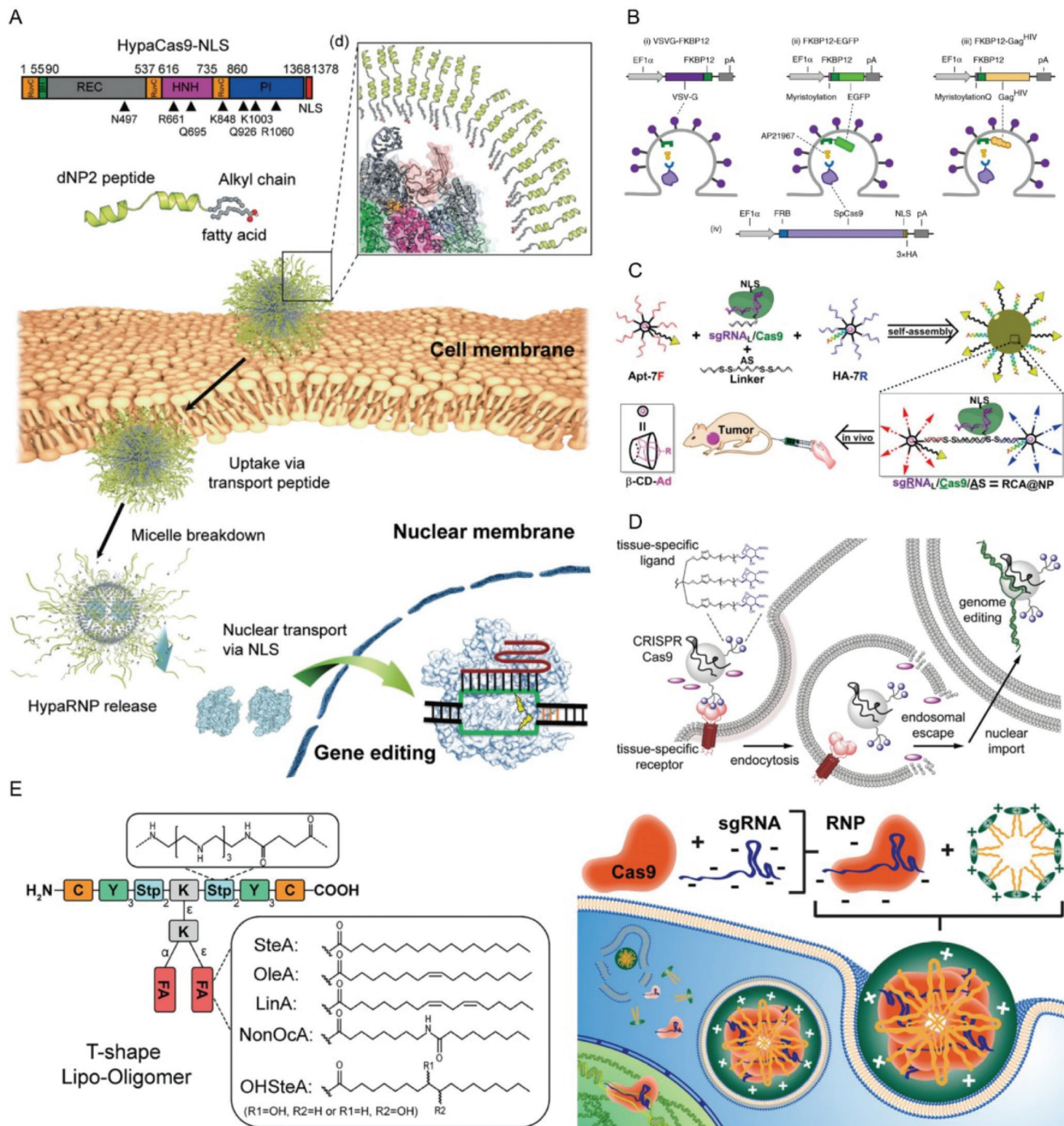


**Fig. 10** Representative delivery systems for Cas9 RNPs. (A) Blood–brain barrier-permeable dNP2-lipopeptide system for delivery of HypaCas9 RNPs. Reproduced with permission from ref. 236. Copyright 2019 American Chemical Society. (B) Extracellular nanovesicle-based Cas9 RNP delivery system. Reproduced with permission from ref. 241. Copyright 2020 Springer Nature. (C) Branched DNA-based delivery system for Cas9 RNP/antisense codelivery. Reproduced with permission from ref. 249. Copyright 2019 American Chemical Society. (D) Cas9 conjugate with trimeric *N*-acetyl galactosamine (GalNAc) ligands for asiaglycoprotein receptor-specific delivery. Reproduced with permission from ref. 251. Copyright 2018 American Chemical Society. (E) Lipo-oligoamino amides for Cas9/sgRNA RNP delivery. Reproduced with permission from ref. 84. Copyright 2020 American Chemical Society. Permission requests related to the material should be directed to the ACS.

ture contain a cationizable hydrophilic backbone, flanking tyrosine trimers and fatty acid modifications (lipo-OAA).<sup>84</sup> These lipo-OAAs were demonstrated to form nanoparticles

with Cas9/sgRNA without disturbing the integrity of the RNP complex. The systematic variation of fatty acid residues (stearic acid, oleic acid, linoleic acid, nonanamidoctanoic acid, hydro-

stearic acid) (Fig. 10E) revealed a particular importance of this structural element for the editing efficiency. The lipo-OAA which contains hydroxy-stearic acid outperformed all analogues, inducing up to 40% EGFP knockout in Neuro2a cells and up to 89% knockout in HeLa cells. Montenegro and collaborators reported cellular delivery of Cas9 by amphiphilic peptides which were synthesized *via* hydrazone bond formation between a cationic peptide (Ac-RRLKRLRLKRL-NH<sub>2</sub>) and hydrophobic aldehyde tails.<sup>238</sup> It was found that oleic aldehyde bound peptides (PT24) achieved the best EGFP disruption efficiency.

**Bio-derived vesicles.** In recent years, great interest has aroused to construct bio-derived vesicles for Cas9 RNP delivery. Montagna *et al.* developed vesicular stomatitis virus fusogenic glycoprotein decorated vesicles (VEsiCas), which demonstrated high transfection efficiency and low toxicity in target cells.<sup>239</sup> The study indicated that VEsiCas enabled genome editing in the cardiac muscles of mice and was able to target multiple genome loci. In another study, Campbell *et al.* produced gesicles by expression of vesicular stomatitis virus glycoprotein with packaged Cas9 RNPs as the cargo.<sup>240</sup> Gesicles with Cas9/sgRNA RNPs targeting the HIV long terminal repeat (LTR) could efficiently edit the LTR region of HIV-NanoLuc CHME-5 cells, which resulted in reduced proviral activity. Using two different homing mechanisms, Gee *et al.* developed an all-in-one Cas9 RNP delivery system named NanoMEDIC with significantly enhanced RNP packaging capacity (Fig. 10B).<sup>241</sup> Specifically, Cas9 protein was loaded into extracellular nanovesicles through chemical induced dimerization and sgRNA was released into vesicles *via* a viral RNA packaging signal and two self-cleaving riboswitches. It was demonstrated that NanoMEDIC induced over 90% DMD exon skipping by disruption of splicing regulatory sites in skeletal muscle cells *in vitro* and permanent genomic exon skipping in mdx mice *in vivo*. Other RNP loading strategies which were reported make use of the specific interaction of RNA aptamers and aptamer-binding proteins (ABP) or the high binding affinity between GFP and GFP nanobodies.<sup>242,243</sup> Recently, Zhuang *et al.* developed EVs that were modified with DNA aptamer-conjugated tetrahedral DNA nanostructures (TDNs) *via* cholesterol anchoring for cell-selective delivery of Cas9 RNPs.<sup>244</sup> The targeting efficiency of different ratios of aptamer/cholesterol were evaluated and it was found that TDNs with 1 : 3 ratio of aptamer/cholesterol increased the accumulation of EVs in HepG2 cells, human primary liver cancer-derived organoids and xenograft tumor models which could be utilized for WNT10B gene disruption with significant tumor growth suppression.

Apart from extracellular vesicles, virus-like particles were reported for Cas9 RNP delivery as another class of bio-derived vehicles. Mangeot *et al.* fabricated murine leukemia virus (MLV)-like particles to encapsulate Cas9 RNPs.<sup>245</sup> The obtained nanoblades induced efficient genome editing in multiple primary cell lines and enabled genome editing in mouse embryos and livers. Doudna and colleagues demonstrated that HIV envelope glycoprotein-pseudotyped Cas9-VLPs could selectively edit genomes in CD4<sup>+</sup> T cells.<sup>246</sup>

**DNA-based delivery systems.** Based on the principle of complementary base pairing, various types of DNA-based delivery systems were created for the delivery of Cas9 RNPs. Sun *et al.* reported the first example of DNA nanoclews (DNA NCs) which were synthesized *via* a rolling circle amplification (RCA).<sup>247</sup> The designed DNA NCs bound to the guide segment of Cas9/sgRNA due to their partially complementary sequences. The obtained Cas9/sgRNA/NC was further coated with PEI (Cas9/sgRNA/NC/PEI) for enhancement of the endosomal escape. After intratumoral injection, Cas9/sgRNA/NC/PEI induced ~25% EGFP disruption at the tumor site. Instead of using PEI, Ding *et al.* generated a non-cationic cross-linked DNA nanogel for Cas9 RNP encapsulation and delivery. Specifically, DNA which is complementary to the tail of sgRNA was firstly grafted on PCL to obtain DNA-g-PCL. After binding of the DNA to Cas9/sgRNA, the residual DNA sequences were cross-linked with DNA *via* hybridization to obtain nanogel-Cas9/sgRNA.<sup>248</sup> *In vitro* transfection showed that the nanogel-Cas9/sgRNA achieved 21.1% reduction of EGFP fluorescence intensity. Recently, Liu *et al.* designed a branched DNA-based multifunctional system for co-delivery of Cas9 RNPs and anti-sense oligonucleotides (Fig. 10C).<sup>249</sup> By simultaneous targeting DNA in the nucleus and mRNA in the cytoplasm, the resultant DNA nanocomplexes induced efficient down regulation of Plk1 gene and thus resulted in remarkable synergistic antitumoral effects. Besides, stimuli-responsive DNA nanoflowers (DNF) were developed by Shi and co-workers for cell-type-specific genome editing.<sup>250</sup> The designed DNA sequences included DNA aptamers with specificity for tumor cells and miR-21 responsive elements for miRNA-triggered Cas9 RNP release. Compared to non-responsive nanoparticles, the established DNF exhibited enhanced knockout efficiency, resulting in significant suppression of EGFP expression in tumor-bearing mice after intratumoral injection.

**Other delivery systems.** The asialoglycoprotein receptor (ASGPR), which is predominantly expressed by hepatocytes, is a well-established target receptor for specific delivery to the liver. Rouet *et al.* designed direct Cas9 conjugates with trimeric ligands of the ASGPR to realize cell-specific delivery of RNPs and genome editing without requirement for an additional delivery system (Fig. 10D).<sup>251</sup> Cas9-ASGPrL showed increased uptake into HepG2 cells due to receptor-mediated endocytosis and genome modification was observed in the presence of endosomolytic peptides. He *et al.* reported a multi-armed amphiphilic cyclodextrin (CDEH)-based delivery system for protein delivery. They demonstrated that CDEH could self-assemble with proteins in aqueous environment to form nanoparticles.<sup>252</sup> After further modification with folate ligands *via* host-guest interactions, the folate-targeted CDEH achieved 47.1% Plk1 gene deletion and 64.1% Plk1 protein reduction, which led to efficient inhibition of HeLa tumor growth *in vivo*. Recently, protein-based delivery systems for Cas9 RNPs were reported. Qiao *et al.* fabricated a chitosan-coated red fluorescent protein (RFP@CS) core for binding E-tagged Cas9 RNPs and a ssDNA template.<sup>253</sup> The RFP@CS nanoparticles could not only serve as a fluorescent probe but also enabled

HDR-editing *in vitro*. Besides, Zhu *et al.* reported the first example of a DNAzyme-controlled editing system based on a Y-shaped DNA, biotin–streptavidin interaction and a DNAzyme which releases Cas9 RNPs upon exposure to Mn<sup>2+</sup>.<sup>254</sup> Pan *et al.* developed a tetralysine-conjugated H-chain apoferritin (TL-HFn) system for packaging and delivery of Cas9 RNPs. The TL-HFn systems delivered Cas9 RNP into the target cells through TfR1-mediated endocytosis and induced EGFP disruption both *in vitro* and *in vivo*.<sup>255</sup>

## Current clinical trials of CRISPR/Cas

Although numerous delivery technologies and Cas9 variants were developed and scientists from industry as well as academia have put much efforts into the translation of these technologies, the clinical application of the CRISPR/Cas systems is still at an early stage. Generally, *ex vivo* and *in vivo* therapies can be discriminated, depending on the genome editing procedure occurring externally or internally of the human body. T cells, CAR-T cells, lymphocytes, hematopoietic stem and progenitor cells (HSPCs), induced pluripotent stem cells (iPSCs) and induced hepatic stem cells (iHSCs) are cell types of particular interest in current *ex vivo* applications.<sup>118</sup> The native cells are isolated from patients, engineered by genomic modifications and then re-infused into the patients. In 2016, the first CRISPR clinical trial of PD-1 edited T cells in patients with advanced non-small-cell lung cancer (NCT02793856) started at the West China Hospital, Sichuan University. The researchers reported that T cells edited by nucleofection with Cas9 plasmids were generally safe for patients and off-target effects were observed at a low level.<sup>256</sup> However, the desired responses were not observed in the patients, which may be due to insufficient T cell expansion, lack of antigen specificity or low editing efficiency. To improve this, several CRISPR-based *ex vivo* clinical trials using Cas9 mRNA or Cas9 RNPs as well as combinations with chimeric antigen receptor T cell (CAR-T) therapies are under investigation (NCT03166878, NCT03398967, NCT03545815, NCT03747965 and NCT04037566). Besides engineered T cells and CAR-T cells, modification of CCR5, BCL11A or mutant HBB in hematopoietic stem and progenitor cells (HSPCs) for treating hematologic diseases using CRISPR/Cas9 systems are in development.<sup>257</sup> In contrast to *ex vivo* applications, where physical methods such as electroporation or nucleofection are feasible approaches to deliver the CRISPR/Cas9 systems, for *in vivo* applications, viral or non-viral vectors are generally required. The first *in vivo* administration of the CRISPR/Cas9 system to humans was conducted with EDIT-101, an AAV5 vector encoding for SaCas9 and two sgRNAs to mediate deletion of a mutated intronic sequence of the CPE290 gene (IVS26) after subretinal injections in patients suffering from Leber's Congenital Amaurosis Type 10.<sup>258</sup> In the ongoing single ascending dose study, 18 participants with LCA10-IVS26 are treated with EDIT-101 (NCT03872479). As discussed above, lipid nanoparticles are used in the first systemically administered CRISPR therapy NTLA-2001 in patients with

hereditary transthyretin amyloidosis with polyneuropathy (NCT04601051). An interim report of the ongoing phase 1 clinical study showed an impressive mean reduction of serum TTR protein by 87% in patients who received a single treatment of NTLA-2001 at a dose of 0.3 mg kg<sup>-1</sup>, which can be considered a first clinical demonstration of safe and efficient direct *in vivo* genome editing in humans.<sup>119</sup>

## Conclusions

Introduction of the CRISPR/Cas9 system into cells can be achieved by using different biomolecular formats. The delivery of DNA, mRNA and RNP introduces the components at different stages of the cellular flow of genetic information. This results in different kinetics and availability of the protein and RNA components required for assembly into the final Cas9/gRNA RNP complex. In the cases of DNA and RNA delivery, one or both CRISPR components are produced by the cellular machinery, which results in an unpreventable latency between the availabilities of gRNA and Cas9. RNP delivery represents the most direct strategy to introduce the pre-assembled and immediately functional CRISPR/Cas9 system into cells, which generally results in higher genome editing efficiency compared to the other biomolecular formats. RNPs are also more rapidly eliminated, since no genetic 'blue-prints' can provide additional supply after the complete dose has been applied. In this regard, a short persistence of the CRISPR/Cas system after the intended gene editing event has occurred is generally desirable to prevent unintended off-target effects. In terms of immunogenicity, the different biomolecular formats also exhibit individual characteristics: while pDNA and mRNA mainly trigger innate immune responses, depending on the presence of bacterial backbone elements or nucleotide sequences, the Cas9 protein can provoke adaptive immune reactions. Due to the outstanding therapeutic potential of the CRISPR/Cas9 system, researchers around the world have worked on numerous delivery strategies based on polymeric, lipidic, inorganic, bioderived and other materials for each of the biomolecular formats. Table S1† (pDNA), Table S2† (RNA) and Table S3† (RNPs) give an overview over the research field, including those publications which are not described in the main part of the article. An interesting observation is the currently differing number of delivery strategies which can be found in the literature for the different biomolecular formats. A high number of pDNA based systems is not surprising, since plasmids were the first format being available for the utilisation of the CRISPR/Cas system and pDNA transfecting agents have a long tradition. Despite the obvious high clinical potential of RNA delivery, which has impressively been demonstrated by the mRNA COVID-19 vaccines and the first clinical trial of systemic CRISPR/Cas9 *in vivo* genome editing,<sup>119</sup> the number of CRISPR RNA publications is the lowest. In contrast, a very high number of research articles on Cas9 RNP delivery demonstrates the high interest, and it is likely to become one preferred delivery strategy, at least for certain applications.



This is attributed to the aspects, that Cas9/sgRNA RNPs exhibit several advantages, as described in the article. In addition, Cas9 RNPs represent a very special case where non-covalent ionic interactions enable robust encapsulation of the protein complexes and efficient delivery is possible similar to nucleic acid transfections. Based on these considerations and the characteristics of the different biomolecular formats, it is expected that especially the research on RNA and RNP delivery will continue to increase extensively with high impact on future therapies.

## Author contributions

Yi Lin: Investigation, writing – original draft. Ernst Wagner: Conceptualization, supervision, writing – original draft. Ulrich Lächelt: Conceptualization, supervision, writing – original draft.

## Conflicts of interest

There are no conflicts of interest to declare.

## Acknowledgements

The authors thank Joachim Rädler and Katrien Remaut for fruitful and inspiring discussions. The authors acknowledge support of their own related research by the UPGRADE (Unlocking Precision Gene Therapy) project that has received funding from the European Union's Horizon 2020 research and innovation programme under grant agreement no. 825825. Y. L. appreciates the fellowship of the China Scholarship Council that supports his Ph.D. study at the LMU Munich, Germany.

## References

- 1 F. J. M. Mojica, C. s. Díez-Villaseñor, J. García-Martínez and E. Soria, *J. Mol. Evol.*, 2005, **60**, 174–182.
- 2 M. Jinek, K. Chylinski, I. Fonfara, M. Hauer, J. A. Doudna and E. Charpentier, *Science*, 2012, **337**, 816–821.
- 3 E. Charpentier and J. A. Doudna, *Nature*, 2013, **495**, 50–51.
- 4 J. D. Sander and J. K. Joung, *Nat. Biotechnol.*, 2014, **32**, 347–355.
- 5 T. Gaj, C. A. Gersbach and C. F. Barbas, *Trends Biotechnol.*, 2013, **31**, 397–405.
- 6 C. Maucksch, B. Connor and C. Rudolph, *Minicircle and Miniplasmid DNA Vectors*, 2013, pp. 59–69, DOI: 10.1002/9783527670420.ch5.
- 7 K. Remaut, N. N. Sanders, F. Fayazpour, J. Demeester and S. C. De Smedt, *J. Controlled Release*, 2006, **115**, 335–343.
- 8 D. Kobelt, M. Schleef, M. Schmeer, J. Aumann, P. M. Schlag and W. Walther, *Mol. Biotechnol.*, 2013, **53**, 80–89.
- 9 A. K. Levacic, S. Morys, S. Kempfer, U. Lächelt and E. Wagner, *Hum. Gene Ther.*, 2017, **28**, 862–874.
- 10 C. Leonhardt, G. Schwake, T. R. Stögbauer, S. Rappl, J.-T. Kuhr, T. S. Ligon and J. O. Rädler, *Nanomedicine*, 2014, **10**, 679–688.
- 11 S. Brunner, T. Sauer, S. Carotta, M. Cotten, M. Saltik and E. Wagner, *Gene Ther.*, 2000, **7**, 401–407.
- 12 K. Remaut, N. Symens, B. Lucas, J. Demeester and S. C. De Smedt, *J. Controlled Release*, 2014, **179**, 1–9.
- 13 M. Ferizi, C. Leonhardt, C. Meggle, M. K. Aneja, C. Rudolph, C. Plank and J. O. Rädler, *Lab Chip*, 2015, **15**, 3561–3571.
- 14 C. E. Smull, M. F. Mallette and E. H. Ludwig, *Biochem. Biophys. Res. Commun.*, 1961, **5**, 247–249.
- 15 A. Vaheri and J. S. Pagano, *Virology*, 1965, **27**, 434–436.
- 16 J. A. Wolff, R. W. Malone, P. Williams, W. Chong, G. Acsadi, A. Jani and P. L. Felgner, *Science*, 1990, **247**, 1465–1468.
- 17 J. Nelson, E. W. Sorensen, S. Mintri, A. E. Rabideau, W. Zheng, G. Besin, N. Khatwani, S. V. Su, E. J. Miracco, W. J. Issa, S. Hoge, M. G. Stanton and J. L. Joyal, *Sci. Adv.*, 2020, **6**, eaaz6893.
- 18 D. Weissman, *Expert Rev. Vaccines*, 2015, **14**, 265–281.
- 19 H. Zhang, K. Rombouts, L. Raes, R. Xiong, S. C. De Smedt, K. Braeckmans and K. Remaut, *Adv. Biosyst.*, 2020, **4**, 2000057.
- 20 M. S. D. Kormann, G. Hasenpusch, M. K. Aneja, G. Nica, A. W. Flemmer, S. Herber-Jonat, M. Huppmann, L. E. Mays, M. Illenyi, A. Schams, M. Griese, I. Bittmann, R. Handgretinger, D. Hartl, J. Rosenecker and C. Rudolph, *Nat. Biotechnol.*, 2011, **29**, 154–157.
- 21 P. S. Kowalski, A. Rudra, L. Miao and D. G. Anderson, *Mol. Ther.*, 2019, **27**, 710–728.
- 22 P. Heissig, W. Schrimpf, P. Hadwiger, E. Wagner and D. C. Lamb, *PLoS One*, 2017, **12**, e0173401.
- 23 W. Chen, J. M. Smeekens and R. Wu, *Chem. Sci.*, 2016, **7**, 1393–1400.
- 24 O. Boussif, F. h. Lezoualc, M. A. Zanta, M. D. Mergny, D. Scherman, B. Demeneix and J. P. Behr, *Proc. Natl. Acad. Sci. U. S. A.*, 1995, **92**, 7297.
- 25 H. Uchida, K. Miyata, M. Oba, T. Ishii, T. Suma, K. Itaka, N. Nishiyama and K. Kataoka, *J. Am. Chem. Soc.*, 2011, **133**, 15524–15532.
- 26 D. Schaffert, C. Troiber, E. E. Salcher, T. Fröhlich, I. Martin, N. Badgumar, C. Dohmen, D. Edinger, R. Kläger, G. Maiwald, K. Farkasova, S. Seeber, K. Jahn-Hofmann, P. Hadwiger and E. Wagner, *Angew. Chem., Int. Ed.*, 2011, **50**, 8986–8989.
- 27 H. Uchida, K. Itaka, T. Nomoto, T. Ishii, T. Suma, M. Ikegami, K. Miyata, M. Oba, N. Nishiyama and K. Kataoka, *J. Am. Chem. Soc.*, 2014, **136**, 12396–12405.
- 28 U. Lächelt, P. Kos, F. M. Mickler, A. Herrmann, E. E. Salcher, W. Rödl, N. Badgumar, C. Bräuchle and E. Wagner, *Nanomedicine*, 2014, **10**, 35–44.
- 29 A. Jarzębińska, T. Pasewald, J. Lambrecht, O. Mykhaylyk, L. Kümmerling, P. Beck, G. Hasenpusch, C. Rudolph,



C. Plank and C. Dohmen, *Angew. Chem., Int. Ed.*, 2016, **55**, 9591–9595.

30 P. Heller, D. Hobernik, U. Lächelt, M. Schinnerer, B. Weber, M. Schmidt, E. Wagner, M. Bros and M. Barz, *J. Controlled Release*, 2017, **258**, 146–160.

31 L. Beckert, L. Kostka, E. Kessel, A. Krhac Levacic, H. Kostkova, T. Etrych, U. Lächelt and E. Wagner, *Eur. J. Pharm. Biopharm.*, 2016, **105**, 85–96.

32 G. Gregoriadis and R. A. Buckland, *Nature*, 1973, **244**, 170–172.

33 G. Weissmann, D. Bloomgarden, R. Kaplan, C. Cohen, S. Hoffstein, T. Collins, A. Gotlieb and D. Nagle, *Proc. Natl. Acad. Sci. U. S. A.*, 1975, **72**, 88.

34 M. Becker-Hapak, S. S. McAllister and S. F. Dowdy, *Methods*, 2001, **24**, 247–256.

35 N. Nischan, H. D. Herce, F. Natale, N. Bohlke, N. Budisa, M. C. Cardoso and C. P. R. Hackenberger, *Angew. Chem., Int. Ed.*, 2015, **54**, 1950–1953.

36 X. Liu, P. Zhang, W. Rödl, K. Maier, U. Lächelt and E. Wagner, *Mol. Pharm.*, 2017, **14**, 1439–1449.

37 G. H. Gao, M. J. Park, Y. Li, G. H. Im, J.-H. Kim, H. N. Kim, J. W. Lee, P. Jeon, O. Y. Bang, J. H. Lee and D. S. Lee, *Biomaterials*, 2012, **33**, 9157–9164.

38 R. Tang, C. S. Kim, D. J. Solfield, S. Rana, R. Mout, E. M. Velázquez-Delgado, A. Chompoosor, Y. Jeong, B. Yan, Z.-J. Zhu, C. Kim, J. A. Hardy and V. M. Rotello, *ACS Nano*, 2013, **7**, 6667–6673.

39 P. Zhang, B. Steinborn, U. Lächelt, S. Zahler and E. Wagner, *Biomacromolecules*, 2017, **18**, 2509–2520.

40 Y.-H. Lin, Y.-P. Chen, T.-P. Liu, F.-C. Chien, C.-M. Chou, C.-T. Chen and C.-Y. Mou, *ACS Appl. Mater. Interfaces*, 2016, **8**, 17944–17954.

41 J.-S. Lim, K. Lee, J.-N. Choi, Y.-K. Hwang, M.-Y. Yun, H.-J. Kim, Y. S. Won, S.-J. Kim, H. Kwon and S. Huh, *Nanotechnology*, 2012, **23**, 085101.

42 Y. Lee, T. Ishii, H. Cabral, H. J. Kim, J.-H. Seo, N. Nishiyama, H. Oshima, K. Osada and K. Kataoka, *Angew. Chem., Int. Ed.*, 2009, **48**, 5309–5312.

43 R. Mout, M. Ray, T. Tay, K. Sasaki, G. Y. Tonga and V. M. Rotello, *ACS Nano*, 2017, **11**, 6416–6421.

44 J. A. Zuris, D. B. Thompson, Y. Shu, J. P. Guilinger, J. L. Bessen, J. H. Hu, M. L. Maeder, J. K. Joung, Z.-Y. Chen and D. R. Liu, *Nat. Biotechnol.*, 2015, **33**, 73–80.

45 L. Cong, F. A. Ran, D. Cox, S. Lin, R. Barretto, N. Habib, P. D. Hsu, X. Wu, W. Jiang, L. A. Marraffini and F. Zhang, *Science*, 2013, **339**, 819–823.

46 J. B. Miller, S. Zhang, P. Kos, H. Xiong, K. Zhou, S. S. Perelman, H. Zhu and D. J. Siegwart, *Angew. Chem.*, 2017, **129**, 1079–1083.

47 H. Kwon, M. Kim, Y. Seo, Y. S. Moon, H. J. Lee, K. Lee and H. Lee, *Biomaterials*, 2018, **156**, 172–193.

48 Y. Furuchi, *Proc. Jpn. Acad., Ser. B*, 2015, **91**, 394–409.

49 A. Roers, B. Hiller and V. Hornung, *Immunity*, 2016, **44**, 739–754.

50 D. J. Goss and F. E. Kleiman, *Wiley Interdiscip. Rev.: RNA*, 2013, **4**, 167–179.

51 A. Wadhwa, A. Aljabbari, A. Lokras, C. Foged and A. Thakur, *Pharmaceutics*, 2020, **12**, 102.

52 D. Kawaguchi, A. Kodama, N. Abe, K. Takeuchi, F. Hashiya, F. Tomoike, K. Nakamoto, Y. Kimura, Y. Shimizu and H. Abe, *Angew. Chem., Int. Ed.*, 2020, **59**, 17403–17407.

53 U. Sahin, K. Karikó and Ö. Türeci, *Nat. Rev. Drug Discovery*, 2014, **13**, 759–780.

54 J. Devoldere, H. Dewitte, S. C. De Smedt and K. Remaut, *Drug Discovery Today*, 2016, **21**, 11–25.

55 K. Karikó, H. Muramatsu, F. A. Welsh, J. Ludwig, H. Kato, S. Akira and D. Weissman, *Mol. Ther.*, 2008, **16**, 1833–1840.

56 S. Vaidyanathan, K. T. Azizian, A. A. Haque, J. M. Henderson, A. Hendel, S. Shore, J. S. Antony, R. I. Hogrefe, M. S. Kormann, M. H. Porteus and A. P. McCaffrey, *Mol. Ther. – Nucleic Acids*, 2018, **12**, 530–542.

57 L. Warren, P. D. Manos, T. Ahfeldt, Y.-H. Loh, H. Li, F. Lau, W. Ebina, P. K. Mandal, Z. D. Smith, A. Meissner, G. Q. Daley, A. S. Brack, J. J. Collins, C. Cowan, T. M. Schlaeger and D. J. Rossi, *Cell Stem Cell*, 2010, **7**, 618–630.

58 A. Thess, S. Grund, B. L. Mui, M. J. Hope, P. Baumhof, M. Fotin-Mleczek and T. Schlake, *Mol. Ther.*, 2015, **23**, 1456–1464.

59 E. Giuliani, C. Piovan, S. Bossi, S. Corna, C. Scavullo, M. Pema, T. Di Tomaso, P. Genovese, A. Lombardo, L. Naldini, C. Bordignon, G. P. Rizzardi and C. Bovolenta, *Mol. Ther.*, 2016, **24**, S53–S54.

60 S. A. Scaringe, *Methods*, 2001, **23**, 206–217.

61 D. J. Dellinger, Z. Timár, J. Myerson, A. B. Sierchala, J. Turner, F. Ferreira, Z. n. Kupihár, G. Dellinger, K. W. Hill, J. A. Powell, J. R. Sampson and M. H. Caruthers, *J. Am. Chem. Soc.*, 2011, **133**, 11540–11556.

62 N. Pardi, M. J. Hogan, F. W. Porter and D. Weissman, *Nat. Rev. Drug Discovery*, 2018, **17**, 261–279.

63 Q. Chen, Y. Zhang and H. Yin, *Adv. Drug Delivery Rev.*, 2021, **168**, 246–258.

64 Y. Liu, E. Holmstrom, J. Zhang, P. Yu, J. Wang, M. A. Dyba, D. Chen, J. Ying, S. Lockett, D. J. Nesbitt, A. R. Ferré-D'Amaré, R. Sousa, J. R. Stagno and Y.-X. Wang, *Nature*, 2015, **522**, 368–372.

65 S. Kim, T. Koo, H.-G. Jee, H.-Y. Cho, G. Lee, D.-G. Lim, H. S. Shin and J.-S. Kim, *Genome Res.*, 2018, **28**, 367–373.

66 W. Mu, N. Tang, C. Cheng, W. Sun, X. Wei and H. Wang, *Protein Cell*, 2019, **10**, 461–465.

67 B. Wienert, J. Shin, E. Zelin, K. Pestal and J. E. Corn, *PLoS Biol.*, 2018, **16**, e2005840.

68 D. Allen, M. Rosenberg and A. Hendel, *Front. Genome Ed.*, 2021, **2**, 617910.

69 S. M. A. Rahman, S. Seki, S. Obika, H. Yoshikawa, K. Miyashita and T. Imanishi, *J. Am. Chem. Soc.*, 2008, **130**, 4886–4896.

70 M. Basila, M. L. Kelley and A. v. B. Smith, *PLoS One*, 2017, **12**, e0188593.



71 J. D. Finn, A. R. Smith, M. C. Patel, L. Shaw, M. R. Youniss, J. van Heteren, T. Dirstine, C. Ciullo, R. Lescarbeau, J. Seitzer, R. R. Shah, A. Shah, D. Ling, J. Growe, M. Pink, E. Rohde, K. M. Wood, W. E. Salomon, W. F. Harrington, C. Dombrowski, W. R. Strapps, Y. Chang and D. V. Morrissey, *Cell Rep.*, 2018, **22**, 2227–2235.

72 A. Hendel, R. O. Bak, J. T. Clark, A. B. Kennedy, D. E. Ryan, S. Roy, I. Steinfeld, B. D. Lunstad, R. J. Kaiser, A. B. Wilkens, R. Bacchetta, A. Tselenko, D. Dellinger, L. Bruhn and M. H. Porteus, *Nat. Biotechnol.*, 2015, **33**, 985–989.

73 K. S. Manning, A. N. Rao, M. Castro and T. A. Cooper, *ACS Chem. Biol.*, 2017, **12**, 2503–2509.

74 A. Mir, J. F. Alterman, M. R. Hassler, A. J. Debacker, E. Hudgens, D. Echeverria, M. H. Brodsky, A. Khvorova, J. K. Watts and E. J. Sontheimer, *Nat. Commun.*, 2018, **9**, 1–9.

75 M. Rahdar, M. A. McMahon, T. P. Prakash, E. E. Swayze, C. F. Bennett and D. W. Cleveland, *Proc. Natl. Acad. Sci. U. S. A.*, 2015, **112**, E7110–E7117.

76 D. E. Ryan, D. Taussig, I. Steinfeld, S. M. Phadnis, B. D. Lunstad, M. Singh, X. Vuong, K. D. Okochi, R. McCaffrey, M. Olesiak, S. Roy, C. W. Yung, B. Curry, J. R. Sampson, L. Bruhn and D. J. Dellinger, *Nucleic Acids Res.*, 2018, **46**, 792–803.

77 H. Yin, C.-Q. Song, S. Suresh, Q. Wu, S. Walsh, L. H. Rhym, E. Mintzer, M. F. Bolukbasi, L. J. Zhu, K. Kauffman, H. Mou, A. Oberholzer, J. Ding, S.-Y. Kwan, R. L. Bogorad, T. Zatsepin, V. Koteliansky, S. A. Wolfe, W. Xue, R. Langer and D. G. Anderson, *Nat. Biotechnol.*, 2017, **35**, 1179–1187.

78 L. F. Ribeiro, L. F. Ribeiro, M. Q. Barreto and R. J. Ward, *Int. J. Genomics*, 2018, **2018**, 1652567.

79 F. Jiang and J. A. Doudna, *Annu. Rev. Biophys.*, 2017, **46**, 505–529.

80 B. Sun, H. Chen and X. Gao, *J. Controlled Release*, 2021, **337**, 698–717.

81 J. A. Doudna and E. Charpentier, *Science*, 2014, **346**, 1258096.

82 M. Jinek, F. Jiang, D. W. Taylor, S. H. Sternberg, E. Kaya, E. Ma, C. Anders, M. Hauer, K. Zhou, S. Lin, M. Kaplan, A. T. Iavarone, E. Charpentier, E. Nogales and J. A. Doudna, *Science*, 2014, **343**, 1247997.

83 C. Troiber, D. Edinger, P. Kos, L. Schreiner, R. Kläger, A. Herrmann and E. Wagner, *Biomaterials*, 2013, **34**, 1624–1633.

84 J. Kuhn, Y. Lin, A. Krhac Levacic, N. Al Danaf, L. Peng, M. Höhn, D. C. Lamb, E. Wagner and U. Lächelt, *Bioconjugate Chem.*, 2020, **31**, 729–742, DOI: 10.1021/acs.bioconjchem.9b00853.

85 H. Lodish, A. Berk, S. L. Zipursky, P. Matsudaira, D. Baltimore and J. Darnell, *Molecular Cell Biology*, WH Freeman, 4th edn, 2000.

86 A. V. Groll, Y. Levin, M. C. Barbosa and A. P. Ravazzolo, *Biotechnol. Prog.*, 2006, **22**, 1220–1224.

87 S. McLenaghan, J. P. Sarsero and P. A. Ioannou, *Genomics*, 2007, **89**, 708–720.

88 S. H. Boo and Y. K. Kim, *Exp. Mol. Med.*, 2020, **52**, 400–408.

89 T. Wei, Q. Cheng, Y.-L. Min, E. N. Olson and D. J. Siegwart, *Nat. Commun.*, 2020, **11**, 1–12.

90 E. Kouranova, K. Forbes, G. Zhao, J. Warren, A. Bartels, Y. Wu and X. Cui, *Hum. Gene Ther.*, 2016, **27**, 464–475.

91 G. Josipović, V. Zoldoš and A. Vojta, *J. Biotechnol.*, 2019, **301**, 18–23.

92 S. Kim, D. Kim, S. W. Cho, J. Kim and J.-S. Kim, *Genome Res.*, 2014, **24**, 1012–1019.

93 C.-F. Xu, G.-J. Chen, Y.-L. Luo, Y. Zhang, G. Zhao, Z.-D. Lu, A. Czarna, Z. Gu and J. Wang, *Adv. Drug Delivery Rev.*, 2021, **168**, 3–29.

94 X. Liang, J. Potter, S. Kumar, Y. Zou, R. Quintanilla, M. Sridharan, J. Carte, W. Chen, N. Roark, S. Ranganathan, N. Ravinder and J. D. Chesnut, *J. Biotechnol.*, 2015, **208**, 44–53.

95 Z. Tu, W. Yang, S. Yan, A. Yin, J. Gao, X. Liu, Y. Zheng, J. Zheng, Z. Li, S. Yang, S. Li, X. Guo and X.-J. Li, *Sci. Rep.*, 2017, **7**, 42081.

96 S. Yang, S. Li and X.-J. Li, *Cell Rep.*, 2018, **25**, 2653–2659.

97 S. Aschenbrenner, S. M. Kallenberger, M. D. Hoffmann, A. Huck, R. Eils and D. Nioppek, *Sci. Adv.*, 2020, **6**, eaay0187.

98 B. Zetsche, S. E. Volz and F. Zhang, *Nat. Biotechnol.*, 2015, **33**, 139–142.

99 K. M. Davis, V. Pattanayak, D. B. Thompson, J. A. Zuris and D. R. Liu, *Nat. Chem. Biol.*, 2015, **11**, 316–318.

100 Y. Nihongaki, F. Kawano, T. Nakajima and M. Sato, *Nat. Biotechnol.*, 2015, **33**, 755–760.

101 J. P. Guilinger, D. B. Thompson and D. R. Liu, *Nat. Biotechnol.*, 2014, **32**, 577–582.

102 B. P. Kleinstiver, V. Pattanayak, M. S. Prew, S. Q. Tsai, N. T. Nguyen, Z. Zheng and J. K. Joung, *Nature*, 2016, **529**, 490–495.

103 I. M. Slaymaker, L. Gao, B. Zetsche, D. A. Scott, W. X. Yan and F. Zhang, *Science*, 2016, **351**, 84–88.

104 J. S. Chen, Y. S. Dagdas, B. P. Kleinstiver, M. M. Welch, A. A. Sousa, L. B. Harrington, S. H. Sternberg, J. K. Joung, A. Yildiz and J. A. Doudna, *Nature*, 2017, **550**, 407–410.

105 A. Casini, M. Olivieri, G. Petris, C. Montagna, G. Reginato, G. Maule, F. Lorenzin, D. Prandi, A. Romanel, F. Demichelis, A. Inga and A. Cereseto, *Nat. Biotechnol.*, 2018, **36**, 265–271.

106 J. K. Lee, E. Jeong, J. Lee, M. Jung, E. Shin, Y.-h. Kim, K. Lee, I. Jung, D. Kim, S. Kim and J.-S. Kim, *Nat. Commun.*, 2018, **9**, 3048.

107 J. H. Hu, S. M. Miller, M. H. Geurts, W. Tang, L. Chen, N. Sun, C. M. Zeina, X. Gao, H. A. Rees, Z. Lin and D. R. Liu, *Nature*, 2018, **556**, 57–63.

108 F. A. Ran, P. D. Hsu, C.-Y. Lin, J. S. Gootenberg, S. Konermann, A. E. Trevino, D. A. Scott, A. Inoue, S. Matoba, Y. Zhang and F. Zhang, *Cell*, 2013, **154**, 1380–1389.

109 C. T. Charlesworth, P. S. Deshpande, D. P. Dever, J. Camarena, V. T. Lemgart, M. K. Cromer,



C. A. Vakulskas, M. A. Collingwood, L. Zhang, N. M. Bode, M. A. Behlke, B. Dejene, B. Cieniewicz, R. Romano, B. J. Lesch, N. Gomez-Ospina, S. Mantri, M. Pavel-Dinu, K. I. Weinberg and M. H. Porteus, *Nat. Med.*, 2019, **25**, 249–254.

110 H. Hemmi, O. Takeuchi, T. Kawai, T. Kaisho, S. Sato, H. Sanjo, M. Matsumoto, K. Hoshino, H. Wagner, K. Takeda and S. Akira, *Nature*, 2000, **408**, 740–745.

111 S. Vaidyanathan, K. T. Azizian, A. K. M. A. Haque, J. M. Henderson, A. Hendel, S. Shore, J. S. Antony, R. I. Hogrefe, M. S. D. Kormann, M. H. Porteus and A. P. McCaffrey, *Mol. Ther. – Nucleic Acids*, 2018, **12**, 530–542.

112 J. M. Crudele and J. S. Chamberlain, *Nat. Commun.*, 2018, **9**, 3497.

113 V. L. Simhadri, J. McGill, S. McMahon, J. Wang, H. Jiang and Z. E. Sauna, *Mol. Ther. – Methods Clin. Dev.*, 2018, **10**, 105–112.

114 M. Behr, J. Zhou, B. Xu and H. Zhang, *Acta Pharm. Sin. B*, 2021, **11**, 2150–2171.

115 T. Coelho, D. Adams, A. Silva, P. Lozeron, P. N. Hawkins, T. Mant, J. Perez, J. Chiesa, S. Warrington, E. Tranter, M. Munisamy, R. Falzone, J. Harrop, J. Cehelsky, B. R. Bettencourt, M. Geissler, J. S. Butler, A. Sehgal, R. E. Meyers, Q. Chen, T. Borland, R. M. Hutabarat, V. A. Clausen, R. Alvarez, K. Fitzgerald, C. Gamba-Vitalo, S. V. Nochur, A. K. Vaishnaw, D. W. Y. Sah, J. A. Gollob and O. B. Suhr, *N. Engl. J. Med.*, 2013, **369**, 819–829.

116 B. Z. Igyártó, S. Jacobsen and S. Ndeupen, *Curr. Opin. Virol.*, 2021, **48**, 65–72.

117 Z.-Y. He, K. Men, Z. Qin, Y. Yang, T. Xu and Y.-Q. Wei, *Sci. China: Life Sci.*, 2017, **60**, 458–467.

118 Y. Li, Z. Glass, M. Huang, Z.-Y. Chen and Q. Xu, *Biomaterials*, 2020, **234**, 119711.

119 J. D. Gillmore, E. Gane, J. Taubel, J. Kao, M. Fontana, M. L. Maitland, J. Seitzer, D. O'Connell, K. R. Walsh, K. Wood, J. Phillips, Y. Xu, A. Amaral, A. P. Boyd, J. E. Cehelsky, M. D. McKee, A. Schiermeier, O. Harari, A. Murphy, C. A. Kyratsous, B. Zambrowicz, R. Soltys, D. E. Gutstein, J. Leonard, L. Sepp-Lorenzino and D. Lebwohl, *N. Engl. J. Med.*, 2021, **385**, 493–502.

120 J. Guo, T. Wan, B. Li, Q. Pan, H. Xin, Y. Qiu and Y. Ping, *ACS Cent. Sci.*, 2021, **7**(6), 990–1000.

121 J. Gong, H. X. Wang, Y. H. Lao, H. Hu, N. Vatan, J. Guo, T. C. Ho, D. Huang, M. Li, D. Shao and K. W. Leong, *Adv. Mater.*, 2020, **32**, 2003537.

122 A. Noureddine, A. Maestas-Olguin, E. A. Saada, A. E. LaBauve, J. O. Agola, K. E. Baty, T. Howard, J. K. Sabo, C. R. S. Espinoza, J. A. Doudna, J. S. Schoeniger, K. S. Butler, O. A. Negrete, C. J. Brinker and R. E. Serda, *Acta Biomater.*, 2020, **114**, 358–368.

123 Y. Wang, P. K. Shahi, X. Wang, R. Xie, Y. Zhao, M. Wu, S. Roge, B. R. Pattnaik and S. Gong, *J. Controlled Release*, 2021, **336**, 296–309.

124 N. Ryu, M.-A. Kim, D. Park, B. Lee, Y.-R. Kim, K.-H. Kim, J.-I. Baek, W. J. Kim, K.-Y. Lee and U.-K. Kim, *Nanomedicine*, 2018, **14**, 2095–2102.

125 C.-S. Cho, *ISRN Mater. Sci.*, 2012, **2012**, 798247.

126 Z. Zhang, T. Wan, Y. Chen, Y. Chen, H. Sun, T. Cao, Z. Songyang, G. Tang, C. Wu, Y. Ping, F.-J. Xu and J. Huang, *Macromol. Rapid Commun.*, 2019, **40**, 1800068.

127 C. Liang, F. Li, L. Wang, Z.-K. Zhang, C. Wang, B. He, J. Li, Z. Chen, A. B. Shaikh, J. Liu, X. Wu, S. Peng, L. Dang, B. Guo, X. He, D. W. T. Au, C. Lu, H. Zhu, B.-T. Zhang, A. Lu and G. Zhang, *Biomaterials*, 2017, **147**, 68–85.

128 L. Li, L. Song, X. Liu, X. Yang, X. Li, T. He, N. Wang, S. Yang, C. Yu, T. Yin, Y. Wen, Z. He, X. Wei, W. Su, Q. Wu, S. Yao, C. Gong and Y. Wei, *ACS Nano*, 2017, **11**, 95–111.

129 L. Li, Z. Yang, S. Zhu, L. He, W. Fan, W. Tang, J. Zou, Z. Shen, M. Zhang, L. Tang, Y. Dai, G. Niu, S. Hu and X. Chen, *Adv. Mater.*, 2019, **31**, 1901187.

130 Y. Lyu, S. He, J. Li, Y. Jiang, H. Sun, Y. Miao and K. Pu, *Angew. Chem., Int. Ed.*, 2019, **58**, 18197–18201.

131 X. Xu, K. Xie, X.-Q. Zhang, E. M. Pridgen, G. Y. Park, D. S. Cui, J. Shi, J. Wu, P. W. Kantoff, S. J. Lippard, R. Langer, G. C. Walker and O. C. Farokhzad, *Proc. Natl. Acad. Sci. U. S. A.*, 2013, **110**, 18638–18643.

132 Y. Takashima, R. Saito, A. Nakajima, M. Oda, A. Kimura, T. Kanazawa and H. Okada, *Int. J. Pharm.*, 2007, **343**, 262–269.

133 Y.-L. Luo, L.-F. Liang, Y.-J. Gan, J. Liu, Y. Zhang, Y.-N. Fan, G. Zhao, A. Czarna, Z.-D. Lu, X.-J. Du, S. Shen, C.-F. Xu, Z.-X. Lian and J. Wang, *ACS Appl. Mater. Interfaces*, 2020, **12**, 48259–48271.

134 M. Li, Y.-N. Fan, Z.-Y. Chen, Y.-L. Luo, Y.-C. Wang, Z.-X. Lian, C.-F. Xu and J. Wang, *Nano Res.*, 2018, **11**, 6270–6282.

135 Y. Liu, G. Zhao, C.-F. Xu, Y.-L. Luo, Z.-D. Lu and J. Wang, *Biomater. Sci.*, 2018, **6**, 1592–1603.

136 Y.-L. Luo, C.-F. Xu, H.-J. Li, Z.-T. Cao, J. Liu, J.-L. Wang, X.-J. Du, X.-Z. Yang, Z. Gu and J. Wang, *ACS Nano*, 2018, **12**, 994–1005.

137 Y. Liu, Z.-T. Cao, C.-F. Xu, Z.-D. Lu, Y.-L. Luo and J. Wang, *Biomaterials*, 2018, **172**, 92–104.

138 Q. Yang, Y. Zhou, J. Chen, N. Huang, Z. Wang and Y. Cheng, *Int. J. Nanomed.*, 2021, **16**, 185.

139 A. Srivastav, K. Gupta, D. Chakraborty, P. Dandekar and R. Jain, *J. Pharm. Innovation*, 2020, 1–14.

140 D. M. Lynn and R. Langer, *J. Am. Chem. Soc.*, 2000, **122**, 10761–10768.

141 A. Akinc, D. M. Lynn, D. G. Anderson and R. Langer, *J. Am. Chem. Soc.*, 2003, **125**, 5316–5323.

142 H. Deng, S. Tan, X. Gao, C. Zou, C. Xu, K. Tu, Q. Song, F. Fan, W. Huang and Z. Zhang, *Acta Pharm. Sin. B*, 2020, **10**, 358–373.

143 X. Gao, Z. Jin, X. Tan, C. Zhang, C. Zou, W. Zhang, J. Ding, B. C. Das, K. Severinov, I. I. Hitzeroth, P. R. Debata, D. He, X. Ma, X. Tian, Q. Gao, J. Wu, R. Tian, Z. Cui, W. Fan, Z. Huang, C. Cao, Y. Bao, S. Tan and Z. Hu, *J. Controlled Release*, 2020, **321**, 654–668.



144 Y. Rui, D. R. Wilson, K. Sanders and J. J. Green, *ACS Appl. Mater. Interfaces*, 2019, **11**, 10472–10480.

145 Y. Rui, M. Varanasi, S. Mendes, H. M. Yamagata, D. R. Wilson and J. J. Green, *Mol. Ther. – Nucleic Acids*, 2020, **20**, 661–672.

146 H. Gao, M. Elsabahy, E. V. Giger, D. Li, R. E. Prud'homme and J.-C. Leroux, *Biomacromolecules*, 2010, **11**, 889–895.

147 X. Zhang, C. Xu, S. Gao, P. Li, Y. Kong, T. Li, Y. Li, F. J. Xu and J. Du, *Adv. Sci.*, 2019, **6**, 1900386.

148 J.-J. Nie, Y. Liu, Y. Qi, N. Zhang, B. Yu, D.-F. Chen, M. Yang and F.-J. Xu, *J. Controlled Release*, 2021, **333**, 362–373.

149 D. Chuan, T. Jin, R. Fan, L. Zhou and G. Guo, *Adv. Colloid Interface Sci.*, 2019, **268**, 25–38.

150 B.-C. Zhang, P.-Y. Wu, J.-J. Zou, J.-L. Jiang, R.-R. Zhao, B.-Y. Luo, Y.-Q. Liao and J.-W. Shao, *Chem. Eng. J.*, 2020, **393**, 124688.

151 H. Zhang, T. F. Bahamondez-Canas, Y. Zhang, J. Leal and H. D. Smyth, *Mol. Pharm.*, 2018, **15**, 4814–4826.

152 Y. Qi, H. Song, H. Xiao, G. Cheng, B. Yu and F.-J. Xu, *Small*, 2018, **14**, 1803061.

153 Y. Qi, Y. Liu, B. Yu, Y. Hu, N. Zhang, Y. Zheng, M. Yang and F. J. Xu, *Adv. Sci.*, 2020, **7**, 2001424.

154 M. Shao, Y. Qi, D. Sui and F.-J. Xu, *Biomater. Sci.*, 2021, **9**, 7104–7114.

155 H.-X. Wang, Z. Song, Y.-H. Lao, X. Xu, J. Gong, D. Cheng, S. Chakraborty, J. S. Park, M. Li, D. Huang, L. Yin, J. Cheng and K. W. Leong, *Proc. Natl. Acad. Sci. U. S. A.*, 2018, **115**, 4903–4908.

156 Y.-H. Lao, M. Li, M. A. Gao, D. Shao, C.-W. Chi, D. Huang, S. Chakraborty, T.-C. Ho, W. Jiang, H.-X. Wang, S. Wang and K. W. Leong, *Adv. Sci.*, 2018, **5**, 1700540.

157 M. R. Emami, C. S. Young, Y. Ji, X. Liu, E. Mokhonova, A. D. Pyle, H. Meng and M. J. Spencer, *Adv. Ther.*, 2019, **2**, 1900061.

158 L. Zhang, P. Wang, Q. Feng, N. Wang, Z. Chen, Y. Huang, W. Zheng and X. Jiang, *NPG Asia Mater.*, 2017, **9**, e441–e441.

159 C.-S. Wang, C.-H. Chang, T.-Y. Tzeng, A. M.-Y. Lin and Y.-L. Lo, *Nanoscale Horiz.*, 2021, **6**, 729–743.

160 M. Li, H. Xie, Y. Liu, C. Xia, X. Cun, Y. Long, X. Chen, M. Deng, R. Guo, Z. Zhang and Q. He, *J. Controlled Release*, 2019, **304**, 204–215.

161 H. Yin, X. Yuan, L. Luo, Y. Lu, B. Qin, J. Zhang, Y. Shi, C. Zhu, J. Yang, X. Li, M. Jiang, Z. Luo, X. Shan, D. Chen and J. You, *Adv. Sci.*, 2020, **7**, 1903381.

162 C. Li, T. Yang, Y. Weng, M. Zhang, D. Zhao, S. Guo, B. Hu, W. Shao, X. Wang, A. Hussain, X. Liang and Y. Huang, *Bioact. Mater.*, 2021, **9**, 590–601.

163 D. Sun, Z. Sun, H. Jiang, A. M. Vaidya, R. Xin, N. R. Ayat, A. L. Schilb, P. L. Qiao, Z. Han, A. Naderi and Z.-R. Lu, *Bioconjugate Chem.*, 2018, **30**, 667–678.

164 Y. Chen, X. Chen, D. Wu, H. Xin, D. Chen, D. Li, H. Pan, C. Zhou and Y. Ping, *Chem. Mater.*, 2020, **33**, 81–91.

165 H. Tang, X. Xu, Y. Chen, H. Xin, T. Wan, B. Li, H. Pan, D. Li and Y. Ping, *Adv. Mater.*, 2021, **33**, 2006003.

166 X. Chen, Y. Chen, H. Xin, T. Wan and Y. Ping, *Proc. Natl. Acad. Sci. U. S. A.*, 2020, **117**, 2395–2405.

167 Y. Tao, K. Yi, H. Hu, D. Shao and M. Li, *J. Mater. Chem. B*, 2021, **9**, 94–100.

168 X. Xu, O. Koivisto, C. Liu, J. Zhou, M. Miihkinen, G. Jacquemet, D. Wang, J. M. Rosenholm, Y. Shu and H. Zhang, *Adv. Ther.*, 2021, **4**, 2000072.

169 B.-C. Zhang, B.-Y. Luo, J.-J. Zou, P.-Y. Wu, J.-L. Jiang, J.-Q. Le, R.-R. Zhao, L. Chen and J.-W. Shao, *ACS Appl. Mater. Interfaces*, 2020, **12**, 57362–57372.

170 J. Shen, Z. Lu, J. Wang, Q. Hao, W. Ji, Y. Wu, H. Peng, R. Zhao, J. Yang, Y. Li, Z. Shi and X. Zhang, *Adv. Mater.*, 2021, 2101993.

171 A. Poddar, S. Pyreddy, F. Carraro, S. Dhakal, A. Rassell, M. R. Field, T. S. Reddy, P. Falcaro, C. M. Doherty and R. Shukla, *Chem. Commun.*, 2020, **56**, 15406–15409.

172 A. Hasanzadeh, F. Radmanesh, E. S. Hosseini, I. Hashemzadeh, J. Kiani, H. Nourizadeh, M. Naseri, Y. Fatahi, F. Chegini, Z. Madjd, A. Beyzavi, P. S. Kowalski and M. Karimi, *Bioconjugate Chem.*, 2021, **32**, 1875–1887.

173 A. Hasanzadeh, F. Radmanesh, E. S. Hosseini, I. Hashemzadeh, J. Kiani, M. Naseri, H. Nourizadeh, Y. Fatahi, B. K. Y. Azar, B. G. Marani, A. Beyzavi, V. P. Mahabadi and M. Karimi, *Nanomedicine*, 2021, **16**, 1673–1690.

174 Y. Wu, J. Zheng, Q. Zeng, T. Zhang and D. Xing, *Nano Res.*, 2020, **13**, 2399–2406.

175 X. Y. He, X. H. Ren, Y. Peng, J. P. Zhang, S. L. Ai, B. Y. Liu, C. Xu and S. X. Cheng, *Adv. Mater.*, 2020, **32**, 2000208.

176 B.-Y. Liu, X.-Y. He, C. Xu, X.-H. Ren, R.-X. Zhuo and S.-X. Cheng, *ACS Appl. Mater. Interfaces*, 2019, **11**, 23870–23879.

177 B.-Y. Liu, X.-Y. He, C. Xu, L. Xu, S.-L. Ai, S.-X. Cheng and R.-X. Zhuo, *Biomacromolecules*, 2018, **19**, 2957–2968.

178 T. Briolay, T. Petithomme, M. Fouet, N. Nguyen-Pham, C. Blanquart and N. Boisgerault, *Mol. Cancer*, 2021, **20**, 1–24.

179 S. M. Kim, Y. Yang, S. J. Oh, Y. Hong, M. Seo and M. Jang, *J. Controlled Release*, 2017, **266**, 8–16.

180 Q. Xu, Z. Zhang, L. Zhao, Y. Qin, H. Cai, Z. Geng, X. Zhu, W. Zhang, Y. Zhang, J. Tan, J. Wang and J. Zhou, *J. Controlled Release*, 2020, **326**, 455–467.

181 Y. Lin, J. Wu, W. Gu, Y. Huang, Z. Tong, L. Huang and J. Tan, *Adv. Sci.*, 2018, **5**, 1700611.

182 X.-H. Ren, X.-Y. He, B.-Y. Liu, C. Xu and S.-X. Cheng, *ACS Appl. Bio Mater.*, 2020, **3**, 7831–7839.

183 T. Killian, A. Buntz, T. Herlet, H. Seul, O. Mundigl, G. Längst and U. Brinkmann, *Nucleic Acids Res.*, 2019, **47**, e55–e55.

184 W.-J. Cheng, L.-C. Chen, H.-O. Ho, H.-L. Lin and M.-T. Sheu, *Int. J. Nanomed.*, 2018, **13**, 7079.

185 Y. Zhang, S. Shen, G. Zhao, C.-F. Xu, H.-B. Zhang, Y.-L. Luo, Z.-T. Cao, J. Shi, Z.-B. Zhao, Z.-X. Lian and J. Wang, *Biomaterials*, 2019, **217**, 119302.



186 X. Li, Q. Feng, Z. Han and X. Jiang, *Chin. J. Chem. Eng.*, 2021, **38**, 216–220.

187 S. Abbasi, S. Uchida, K. Toh, T. A. Tockary, A. Dirisala, K. Hayashi, S. Fukushima and K. Kataoka, *J. Controlled Release*, 2021, **332**, 260–268.

188 X. Huang, R. Zheng, F. Ding, J. Yang, M. Xie, X. Liu, J. Li, J. Feng, X. Zhu and C. Zhang, *ACS Mater. Lett.*, 2020, **2**, 1509–1515.

189 H. Yin, C.-Q. Song, J. R. Dorkin, L. J. Zhu, Y. Li, Q. Wu, A. Park, J. Yang, S. Suresh, A. Bishanova, A. Gupta, M. F. Bolukbasi, S. Walsh, R. L. Bogorad, G. Gao, Z. Weng, Y. Dong, V. Koteliansky, S. A. Wolfe, R. Langer, W. Xue and D. G. Anderson, *Nat. Biotechnol.*, 2016, **34**, 328–333.

190 C. Jiang, M. Mei, B. Li, X. Zhu, W. Zu, Y. Tian, Q. Wang, Y. Guo, Y. Dong and X. Tan, *Cell Res.*, 2017, **27**, 440–443.

191 J. Liu, J. Chang, Y. Jiang, X. Meng, T. Sun, L. Mao, Q. Xu and M. Wang, *Adv. Mater.*, 2019, **31**, 1902575.

192 Y. Li, R. Jarvis, K. Zhu, Z. Glass, R. Ogurlu, P. Gao, P. Li, J. Chen, Y. Yu, Y. Yang and Q. Xu, *Angew. Chem.*, 2020, **132**, 15067–15074.

193 M. Qiu, Z. Glass, J. Chen, M. Haas, X. Jin, X. Zhao, X. Rui, Z. Ye, Y. Li, F. Zhang and Q. Xu, *Proc. Natl. Acad. Sci. U. S. A.*, 2021, **118**(10), e2020401118.

194 X. Zhao, Z. Glass, J. Chen, L. Yang, D. L. Kaplan and Q. Xu, *Adv. Healthcare Mater.*, 2021, **10**, 2000938.

195 X. Zhang, B. Li, X. Luo, W. Zhao, J. Jiang, C. Zhang, M. Gao, X. Chen and Y. Dong, *ACS Appl. Mater. Interfaces*, 2017, **9**, 25481–25487.

196 Q. Cheng, T. Wei, L. Farbiak, L. T. Johnson, S. A. Dilliard and D. J. Siegwart, *Nat. Nanotechnol.*, 2020, **15**, 313–320.

197 S. Liu, Q. Cheng, T. Wei, X. Yu, L. T. Johnson, L. Farbiak and D. J. Siegwart, *Nat. Mater.*, 2021, **20**, 701–710.

198 L. Farbiak, Q. Cheng, T. Wei, E. Álvarez-Benedicto, L. T. Johnson, S. Lee and D. J. Siegwart, *Adv. Mater.*, 2021, 2006619.

199 D. Rosenblum, A. Gutkin, R. Kedmi, S. Ramishetti, N. Veiga, A. M. Jacobi, M. S. Schubert, D. Friedmann-Morvinski, Z. R. Cohen, M. A. Behlke, J. Lieberman and D. Peer, *Sci. Adv.*, 2020, **6**, eabc9450.

200 Q. Tang, J. Liu, Y. Jiang, M. Zhang, L. Mao and M. Wang, *ACS Appl. Mater. Interfaces*, 2019, **11**, 46585–46590.

201 Z. Chen, F. Liu, Y. Chen, J. Liu, X. Wang, A. T. Chen, G. Deng, H. Zhang, J. Liu, Z. Hong and J. Zhou, *Adv. Funct. Mater.*, 2017, **27**, 1703036.

202 T. Wan, Y. Chen, Q. Pan, X. Xu, Y. Kang, X. Gao, F. Huang, C. Wu and Y. Ping, *J. Controlled Release*, 2020, **322**, 236–247.

203 T. Wan, Q. Pan and Y. Ping, *Sci. Adv.*, 2021, **7**, eabe2888.

204 Q. Ban, P. Yang, S.-J. Chou, L. Qiao, H. Xia, J. Xue, F. Wang, X. Xu, N. Sun, R. Y. Zhang, C. Zhang, A. Lee, W. Liu, T.-Y. Lin, Y.-L. Ko, P. Antovski, X. Zhang, S.-H. Chiou, C.-F. Lee, W. Hui, D. Liu, S. J. Jonas, P. S. Weiss and H.-R. Tseng, *Small*, 2021, **17**, 2100546.

205 Q. Liu, J. Cai, Y. Zheng, Y. Tan, Y. Wang, Z. Zhang, C. Zheng, Y. Zhao, C. Liu, Y. An, C. Jiang, L. Shi, C. Kang and Y. Liu, *Nano Lett.*, 2019, **19**, 7662–7672.

206 S. Deng, X. Li, S. Liu, J. Chen, M. Li, S. Y. Chew, K. W. Leong and D. Cheng, *Sci. Adv.*, 2020, **6**, eabb4005.

207 Y. Rui, D. R. Wilson, J. Choi, M. Varanasi, K. Sanders, J. Karlsson, M. Lim and J. J. Green, *Sci. Adv.*, 2019, **5**, eaay3255.

208 G. Chen, A. A. Abdeen, Y. Wang, P. K. Shahi, S. Robertson, R. Xie, M. Suzuki, B. R. Pattnaik, K. Saha and S. Gong, *Nat. Nanotechnol.*, 2019, **14**, 974–980.

209 C. Liu, T. Wan, H. Wang, S. Zhang, Y. Ping and Y. Cheng, *Sci. Adv.*, 2019, **5**, eaaw8922.

210 R. Kumar, N. Le, Z. Tan, M. E. Brown, S. Jiang and T. M. Reineke, *ACS Nano*, 2020, **14**, 17626–17639.

211 T.-C. Ho, H. S. Kim, Y. Chen, Y. Li, M. W. LaMere, C. Chen, H. Wang, J. Gong, C. D. Palumbo, J. M. Ashton, H.-W. Kim, Q. Xu, M. W. Becker and K. W. Leong, *Sci. Adv.*, 2021, **7**, eabg3217.

212 Y. A. Aksoy, B. Yang, W. Chen, T. Hung, R. P. Kuchel, N. W. Zammit, S. T. Grey, E. M. Goldys and W. Deng, *ACS Appl. Mater. Interfaces*, 2020, **12**, 52433–52444.

213 J.-Y. Ryu, E.-J. Won, H. A. R. Lee, J. H. Kim, E. Hui, H. P. Kim and T.-J. Yoon, *Biomaterials*, 2020, **232**, 119736.

214 K. Lee, M. Conboy, H. M. Park, F. Jiang, H. J. Kim, M. A. Dewitt, V. A. Mackley, K. Chang, A. Rao, C. Skinner, T. Shobha, M. Mehdipour, H. Liu, W.-c. Huang, F. Lan, N. L. Bray, S. Li, J. E. Corn, K. Kataoka, J. A. Doudna, I. Conboy and N. Murthy, *Nat. Biomed. Eng.*, 2017, **1**, 889–901.

215 R. Shahbazi, G. Sghia-Hughes, J. L. Reid, S. Kubek, K. G. Haworth, O. Humbert, H.-P. Kiem and J. E. Adair, *Nat. Mater.*, 2019, **18**, 1124–1132.

216 L. Zhang, L. Wang, Y. Xie, P. Wang, S. Deng, A. Qin, J. Zhang, X. Yu, W. Zheng and X. Jiang, *Angew. Chem., Int. Ed.*, 2019, **58**, 12404–12408.

217 J. Wu, H. Peng, X. Lu, M. Lai, H. Zhang and X. C. Le, *Angew. Chem., Int. Ed.*, 2021, **60**, 11104–11109.

218 Y.-W. Lee, R. Mout, D. C. Luther, Y. Liu, L. Castellanos-García, A. S. Burnside, M. Ray, G. Y. Tonga, J. Hardie, H. Nagaraj, R. Das, E. L. Phillips, T. Tay, R. W. Vachet and V. M. Rotello, *Adv. Ther.*, 2019, **2**, 1900041.

219 X. Li, Y. Pan, C. Chen, Y. Gao, X. Liu, K. Yang, X. Luan, D. Zhou, F. Zeng, X. Han and Y. Song, *Angew. Chem., Int. Ed.*, 2021, **60**, 21200–21204.

220 M. Hansen-Bruhn, B. E. F. de Ávila, M. Beltrán-Gastélum, J. Zhao, D. E. Ramírez-Herrera, P. Angsantikul, K. V. Gothelf, L. Zhang and J. Wang, *Angew. Chem., Int. Ed.*, 2018, **57**, 2657–2661.

221 S. K. Alsaiari, S. Patil, M. Alyami, K. O. Alamoudi, F. A. Aleisa, J. S. Merzaban, M. Li and N. M. Khashab, *J. Am. Chem. Soc.*, 2018, **140**, 143–146.

222 M. Z. Alyami, S. K. Alsaiari, Y. Li, S. S. Qutub, F. A. Aleisa, R. Sougrat, J. S. Merzaban and N. M. Khashab, *J. Am. Chem. Soc.*, 2020, **142**, 1715–1720.

223 X. Yang, Q. Tang, Y. Jiang, M. Zhang, M. Wang and L. Mao, *J. Am. Chem. Soc.*, 2019, **141**, 3782–3786.

224 J. Liu, T. Luo, Y. Xue, L. Mao, P. J. Stang and M. Wang, *Angew. Chem., Int. Ed.*, 2021, **60**, 5429–5435.



225 B. Liu, W. Ejaz, S. Gong, M. Kurbanov, M. Canakci, F. Anson and S. Thayumanavan, *Nano Lett.*, 2020, **20**, 4014–4021.

226 Y. Pan, J. Yang, X. Luan, X. Liu, X. Li, J. Yang, T. Huang, L. Sun, Y. Wang and Y. Lin, *Sci. Adv.*, 2019, **5**, eaav7199.

227 C. Chen, Y. Ma, S. Du, Y. Wu, P. Shen, T. Yan, X. Li, Y. Song, Z. Zha and X. Han, *Small*, 2021, **17**, 2101155.

228 H. Yue, X. Zhou, M. Cheng and D. Xing, *Nanoscale*, 2018, **10**, 1063–1071.

229 W. Zhou, H. Cui, L. Ying and X. F. Yu, *Angew. Chem.*, 2018, **130**, 10425–10429.

230 S. Ramakrishna, A.-B. K. Dad, J. Beloor, R. Gopalappa, S.-K. Lee and H. Kim, *Genome Res.*, 2014, **24**, 1020–1027.

231 J. Yin, Q. Wang, S. Hou, L. Bao, W. Yao and X. Gao, *J. Am. Chem. Soc.*, 2018, **140**, 17234–17240.

232 J. Yin, S. Hou, Q. Wang, L. Bao, D. Liu, Y. Yue, W. Yao and X. Gao, *Bioconjugate Chem.*, 2019, **30**, 898–906.

233 S. M. Kim, S. C. Shin, E. E. Kim, S.-H. Kim, K. Park, S. J. Oh and M. Jang, *ACS Nano*, 2018, **12**, 7750–7760.

234 H. Park, J. Oh, G. Shim, B. Cho, Y. Chang, S. Kim, S. Baek, H. Kim, J. Shin, H. Choi, J. Yoo, J. Kim, W. Jun, M. Lee, C. J. Lengner, Y.-K. Oh and J. Kim, *Nat. Neurosci.*, 2019, **22**, 524–528.

235 S. Krishnamurthy, C. Wohlford-Lenane, S. Kandimalla, G. Sartre, D. K. Meyerholz, V. Théberge, S. Hallée, A.-M. Duperré, T. Del'Guidice, J.-P. Lepetit-Stoffaës, X. Barbeau, D. Guay and P. B. McCray, *Nat. Commun.*, 2019, **10**, 4906.

236 T. T. Thach, D. H. Bae, N. H. Kim, E. S. Kang, B. S. Lee, K. Han, M. Kwak, H. Choi, J. Nam, T. Bae, M. Suh, J. K. Hur and Y. H. Kim, *Small*, 2019, **15**, 1903172.

237 P. K. Jain, J. H. Lo, S. Ranawanare, M. Downing, A. Panda, M. Tai, S. Raghavan, H. E. Fleming and S. N. Bhatia, *Nanoscale*, 2019, **11**, 21317–21323.

238 I. Lostalé-Seijo, I. Louzao, M. Juanes and J. Montenegro, *Chem. Sci.*, 2017, **8**, 7923–7931.

239 C. Montagna, G. Petris, A. Casini, G. Maule, G. M. Franceschini, I. Zanella, L. Conti, F. Arnoldi, O. R. Burrone, L. Zentilin, S. Zacchigna, M. Giacca and A. Cereseto, *Mol. Ther. – Nucleic Acids*, 2018, **12**, 453–462.

240 L. A. Campbell, L. M. Coke, C. T. Richie, L. V. Fortuno, A. Y. Park and B. K. Harvey, *Mol. Ther.*, 2019, **27**, 151–163.

241 P. Gee, M. S. Y. Lung, Y. Okuzaki, N. Sasakawa, T. Iguchi, Y. Makita, H. Hozumi, Y. Miura, L. F. Yang, M. Iwasaki, X. H. Wang, M. A. Waller, N. Shirai, Y. O. Abe, Y. Fujita, K. Watanabe, A. Kagita, K. A. Iwabuchi, M. Yasuda, H. Xu, T. Noda, J. Komano, H. Sakurai, N. Inukai and A. Hotta, *Nat. Commun.*, 2020, **11**, 1334.

242 X. Yao, P. Lyu, K. Yoo, M. K. Yadav, R. Singh, A. Atala and B. Lu, *J. Extracell. Vesicles*, 2021, **10**, e12076.

243 Y. Ye, X. Zhang, F. Xie, B. Xu, P. Xie, T. Yang, Q. Shi, C.-Y. Zhang, Y. Zhang and J. Chen, *Biomater. Sci.*, 2020, **8**, 2966–2976.

244 J. Zhuang, J. Tan, C. Wu, J. Zhang, T. Liu, C. Fan, J. Li and Y. Zhang, *Nucleic Acids Res.*, 2020, **48**, 8870–8882.

245 P. E. Mangeot, V. Risson, F. Fusil, A. Marnef, E. Laurent, J. Blin, V. Mournetas, E. Massouridès, T. J. Sohier, A. Corbin, F. Aubé, M. Teixeira, C. Pinset, L. Schaeffer, G. Legube, F.-L. Cosset, E. Verhoeven, T. Ohlmann and E. P. Ricci, *Nat. Commun.*, 2019, **10**, 1–15.

246 J. R. Hamilton, C. A. Tsuchida, D. N. Nguyen, B. R. Shy, E. R. McGarrigle, C. R. S. Espinoza, D. Carr, F. Blaescke, A. Marson and J. A. Doudna, *Cell Rep.*, 2021, **35**, 109207.

247 W. Sun, W. Ji, J. M. Hall, Q. Hu, C. Wang, C. L. Beisel and Z. Gu, *Angew. Chem.*, 2015, **127**, 12197–12201.

248 F. Ding, X. Huang, X. Gao, M. Xie, G. Pan, Q. Li, J. Song, X. Zhu and C. Zhang, *Nanoscale*, 2019, **11**, 17211–17215.

249 J. Liu, T. Wu, X. Lu, X. Wu, S. Liu, S. Zhao, X. Xu and B. Ding, *J. Am. Chem. Soc.*, 2019, **141**, 19032–19037.

250 J. Shi, X. Yang, Y. Li, D. Wang, W. Liu, Z. Zhang, J. Liu and K. Zhang, *Biomaterials*, 2020, **256**, 120221.

251 R. Rouet, B. A. Thuma, M. D. Roy, N. G. Lintner, D. M. Rubitski, J. E. Finley, H. M. Wisniewska, R. Mendonsa, A. Hirsh, L. de Oñate, J. C. Barrón, T. J. McLellan, J. Bellenger, X. Feng, A. Varghese, B. A. Chrunyk, K. Borzillieri, K. D. Hesp, K. Zhou, N. Ma, M. Tu, R. Dullea, K. F. McClure, R. C. Wilson, S. Liras, V. Mascitti and J. A. Doudna, *J. Am. Chem. Soc.*, 2018, **140**, 6596–6603.

252 X. He, Q. Long, Z. Zeng, L. Yang, Y. Tang and X. Feng, *Adv. Funct. Mater.*, 2019, **29**, 1906187.

253 J. Qiao, W. Sun, S. Lin, R. Jin, L. Ma and Y. Liu, *Chem. Commun.*, 2019, **55**, 4707–4710.

254 X. Zhu, M.-M. Lv, J.-W. Liu, R.-Q. Yu and J.-H. Jiang, *Chem. Commun.*, 2019, **55**, 6511–6514.

255 X. Pan, X. Pei, H. Huang, N. Su, Z. Wu, Z. Wu and X. Qi, *J. Controlled Release*, 2021, **337**, 686–697.

256 Y. Lu, J. Xue, T. Deng, X. Zhou, K. Yu, L. Deng, M. Huang, X. Yi, M. Liang, Y. Wang, H. Shen, R. Tong, W. Wang, L. Li, J. Song, J. Li, X. Su, Z. Ding, Y. Gong, J. Zhu, Y. Wang, B. Zou, Y. Zhang, Y. Li, L. Zhou, Y. Liu, M. Yu, Y. Wang, X. Zhang, L. Yin, X. Xia, Y. Zeng, Q. Zhou, B. Ying, C. Chen, Y. Wei, W. Li and T. Mok, *Nat. Med.*, 2020, **26**, 732–740.

257 E. González-Romero, C. Martínez-Valiente, C. García-Ruiz, R. P. Vázquez-Manrique, J. Cervera and A. Sanjuan-Pla, *Haematologica*, 2019, **104**, 881.

258 News in Brief, *Nat. Biotechnol.*, 2020, **38**, 382–382.

